Incident Light Modulation by Means of Power Variations and Light Pulsing Reduces Photo Induced Toxicity and Bleaching

Firas Mubaid

Department of Physiology,

McGill University, Montreal

A thesis submitted to McGill University in partial fulfillment of the requirements of the degree of Master of Science in Physiology

Thesis Supervisor: Dr. Claire M. Brown

Acknowledgements

This project would not have been successful without the help and support of many people. First, many thanks to Dr. Claire Brown for her guidance and advising throughout the study. Her attitude, patience and morals have been a great inspiration for my self-development, and her flexibility and encouragements have driven the progression of the project. It has been a pleasure to work and learn from her, and it has made for a thrilling graduate experience.

Countless thanks are extended to Colton Boudreau, Rebecca Deagle, Kathy Tang and Abira Rajah of the Brown lab for their invaluable technical and moral support, in addition to their great friendships. Writing of this thesis was done with excellent editorial support from Rebecca Deagle and Abira Rajah. Gratitude is also extended to Dr. Erika Wee who provided imaging training and technical support with outstanding knowledge and capacities. And of course, thank you to the undergraduate students Eva Jin, Jennifer Vo, and Anas Assi for their much-appreciated work and contributions to this project.

Microscopy imaging and data analysis were conducted at the Advanced BioImaging Facility (ABIF) at McGill University. Thank you for the generous donation of CHO-K1-paxillin-EGFP cells by the Rick Horwitz lab at the University of Virginia which were extensively used in this study. Thank you to the Orlowski lab for their assistance in molecular biology techniques. Thank you to Dr. Alvin Shrier, Dr. Anmar Khadra and Dr. Gil Bub for serving on my supervising committee. Immense gratitude to Dr. Gil Bub providing useful discussions and advice on the project, and for lending us experimental tools. Thank you to the Department of Physiology, particularly Rosetta Vasile, for guiding my graduate experience and providing excellent administrative help. Thank you to Nikon and CoolLED for their collaboration with some of the project. And finally, many thanks to my family and friends for their invaluable support throughout this endeavour.

Abstract

The use of fluorescence in microscopy has introduced unprecedented specificity and contrast, paving the way for highly specialized techniques and applications such as correlation mapping or super resolution microscopy for single molecular resolution. However, this powerful tool is curtailed by light damage. Photobleaching of dye molecules causes a gradual loss of signal emission, while phototoxicity causes cell wide disturbances to biological systems and physiological functions. This study introduces novel imaging techniques and recommendations that address these two problems. Chinese Hamster Ovary (CHO-K1) cells complemented with different fluorophores were used to demonstrate the efficiency of the techniques. Phototoxicity levels were evaluated by using the migration and protrusion assays, which measure the speeds of motility and protrusion formation, respectively. The photobleaching assay was used to measure the halftime of signal intensity decay, which provides the speed of photobleaching. This study shows that using low incident light power coupled with long exposure times causes reduced levels of photobleaching and phototoxicity. It also demonstrates that this technique is more efficient at minimizing photodamage than the commercial antifade agent ProLong Live™. Finally, this study shows that pulsing incident light significantly reduces photobleaching. Modulations including the decrease of pulse width, the increase of rest time between pulses, and the decrease of pulse amplitude amplify this effect. This project resulted in the development of several novel imaging techniques that not only considerably reduce light-induced damage but are simple and generally applicable on any fluorescence microscope.

Abrégé

L'utilisation de la fluorescence en microscopie a introduit un niveau de spécificité en détection et un contraste jamais vue auparavant. Cela a permis le développement de techniques hautement spécialisées, tels que l'imagerie corrélative ou la microscopie à super-résolution. Cependant, l'utilisation de cet outil engendre des effets endommageant depuis les ondes utilisées pour l'activation des fluorochromes. Premièrement, le photo-blanchissement des fluorochromes cause une perte graduelle de la fluorescence d'un spécimen. Deuxièmement, la phototoxicité perturbe les systèmes biologiques et les fonctions physiologiques dans une cellule. Cette étude introduit des nouvelles techniques d'imagerie et des recommandations pour minimiser ces méfaits. Des cellules ovariennes de hamster chinois (CHO-K1) supplémentées avec des fluorochromes variés ont étés utilisé pour démontrer l'efficacité de ces techniques. Les mesures des vitesses de motilité, aussi bien que les vitesses auxquelles se forment des saillies sur les membranes cellulaires ont été utilisées pour tester le niveau de phototoxicité durant l'imagerie de cellules vivantes. Le mi-temps de la perte d'intensité de fluorescence a été la mesure du taux de photo-blanchissement dans des cellule fixés. Pour la première technique, cette étude démontre que l'utilisation de puissances de lumière faible accouplée avec des longues périodes d'exposition lumineuse réduit les niveaux de phototoxicités et de photo-blanchissements. De plus, cette technique est plus efficace que l'utilisation d'un produit commerciale, ProLong Live™, à cet effet. Finalement, cette étude démontre que pulser la lumière incidente réduit ses effets endommageant. Cette amélioration est amplifié lorsque la largeur des pulse est réduites, lorsque le temps entre chaque pulse est augmenté, et lorsque l'amplitude (intensité lumineuse) des pulse est réduite. Le résultat de ce projet a été le développement de plusieurs nouvelles techniques d'imagerie qui non seulement réduit les dommages de la lumière, mais qui sont à la fois simple et applicable sur n'importe quel microscope a fluorescence.

Table of Contents

List of Figures

List of Tables

Chapter 1

Introduction

1.1 – Fluorescence microscopy

Since its invention, microscopy has been an invaluable tool that has revolutionised many fields of science. This technology does justice to the ancient adage of "seeing is believing," whereby the human eye can see beyond the macroscopic scale and peer inside the mysteries of the microscopic world. In the late 17th century, Antonie Van Leeuwenhoek designed the first microscope and described the creatures he observed as "animalcules," which we now refer to as microbes[1]. This created a whole new field of study in microbiology, which has exponentially expanded since then. The first and most simple microscopy technique that was developed was brightfield, where light from an incandescent bulb is transmitted through the instrumentation and passes through a sample. Some of this light is partially absorbed by cellular components in the sample, which results in regions of the sample appearing dark against a bright background because the surrounding medium does not contain anything to absorb the illumination. Transmitted light techniques have since considerably evolved to improve sample contrast with several techniques such as darkfield illumination, phase contrast, and differential interference contrast optics[2]. Proceeding these advancements, microscopy revolutionised the field once more at the turn of the 20th century with the dawn of a new, reflected light technique known as fluorescence microscopy[3].

Fluorescence microscopy utilizes a phenomenon known as fluorescence, where specific wavelengths of light are used to visualize molecules of interest, such as proteins. Fluorescence is a form of luminescence, which exploits molecules that can absorb light of a given wavelength and subsequently emit excess energy at a lower energy and longer wavelength of light. This shift in energy causes a difference in what colour of light is used to excite the fluorescent molecule, or fluorophore, and what colour of light is emitted from that molecule. Fluorescence microscopy manipulates this photophysical process to reflect the emitted light from fluorophores within samples to either a set of eyepieces or a camera that is integrated with the microscope to produce an image. High specificity is achieved by coupling different fluorophores to specific molecules of interest, then those will be imaged separately, allowing many different molecules of interest to be resolved within a single sample with high contrast[1].

Widefield fluorescence microscopy is a common application for fluorescence imaging that is affordable, straightforward to use and useful for applications across the physical and life sciences[4]. This

platform of microscopy illuminates a whole field of view at once and employs a camera to collect emitted photons from fluorophores within that field, which allows it to quickly reconstruct a digital image of the fluorescent sample. The downside of this technique is that a large amount of out of focus light is emitted and makes it challenging to resolve fine structures. This is because excitation light passes through the entire sample during illumination and is not limited to the focal plane being imaged. Therefore, fluorophores located in out-of-focus planes also emit light that is detected and integrated by the camera which results in a high background and reduced contrast. One way to circumvent this problem is to use a deconvolution function which employs a mathematical algorithm to subtract light coming from out-of-focus planes from the final image[5]. However, when samples are of more than 20-30 µm in thickness, the amount of out of focus light becomes excessive and a new method of acquisition becomes necessary. Confocal microscopy is fundamentally different from the widefield platform in that it uses a highly focused beam of light, usually a laser, to scan across a sample and sequentially excite fluorophores in the field of view as it passes over them[1]. Light emission then passes through a pinhole aperture which blocks all light coming from out of the focal point of the laser beam. The accepted light is collected by a photomultiplier tube which constructs an image pixel by pixel. A photomultiplier tube can amplify the number of photons as it receives them which confers it an advantage over cameras used in widefield microscopy in that it can electronically enhance weakly fluorescent samples. As such, confocal microscopy can considerably enhance resolution and contrast which is particularly useful in 3D applications, though it does lower sensitivity due to the rejection of a large amount of light coming from out of focus planes.

1.2 – Fluorophores and their photophysical framework

1.2.1 – Photophysics of fluorescence

Fluorescence is part of a complex series of reactions that have yet to be fully understood. For simplified referencing in this text, the photophysical reactions have been numbered in Figure 1.1 which summarizes fluorescence as it is understood today[6-12]. This photophysical process begins with a fluorescent molecule in its relaxed ground energy state absorbing a photon of light with the appropriate quantum energy (Fig. 1.1, Step 1). This excites the molecule and displaces its outermost electron to a higher energetic orbital, and the molecule is then said to be in its singlet excited state. It is important to note, however, that molecules are not necessarily excitable by photons of the same energy level. To excite a molecule, a photon must have an energy amount roughly equivalent to the energy of the transition between the ground state and one of the higher-level excited state orbitals. Evidently, the energy required for this transition is different for different molecules. For instance, the fluorescein isothiocyanate (FITC)

dye is excited with higher energy blue light, whereas the tetramethyl rhodamine (TRITC) dye is excited by lower energy green light. An electron in an excited state orbital is unstable and the molecule will readily release excess energy to return to the ground state through processes such as internal conversion and vibrational relaxation (Fig. 1.1, Step 2). Alternatively, the excited molecule can relax down to the ground state by releasing excess energy in the form of a photon of light. There is partial energy loss in the excited state through molecular vibrations and heat, therefore the wavelength of the emitted photon is always shifted to a lower energy and longer wavelength of light. This phenomenon is termed Stokes shift, and it is harnessed in the design of fluorescence microscopes. The distinction of the excitation light from the emission light is crucial which makes dyes with larger Stokes shifts more desirable. Other than the radiative and non-radiative relaxation pathways to the ground state, a molecule can also undergo the process of intersystem crossing (ISC) into the triplet excited state (Fig. 1.1, Step 3). This is a rare event due to the requirement of a forbidden flip in the spin of the excited electron. Probabilities for these transitions are orders of magnitude smaller than other decay pathways[13]. The lifetime of the triplet excited state is considerably longer than the excited singlet state because the electron requires another rare forbidden flip in its spin to exit the triplet state and relax. Therefore, reactions that can lead to photobleaching and phototoxicity mainly occur from the long-lived triplet state, which will be discussed later in this chapter. The long lifetime of the triplet state also increases the probability of absorption of additional photons when high light powers are applied to a sample. This excess energy can further excite electrons to higher excited state or triplet state orbitals and increase their reactivity. The resulting molecules are highly reactive and have a high probability of secondary reactions with other molecules in the system. Similar to the singlet state, the triplet state can return to the ground state following processes such as vibrational relaxation or emission of light of a much lower energy (i.e. longer wavelength) and slower time scales ($\sim 10^{-3}$s) through the process of phosphorescence (Fig. 1.1, Step 4).

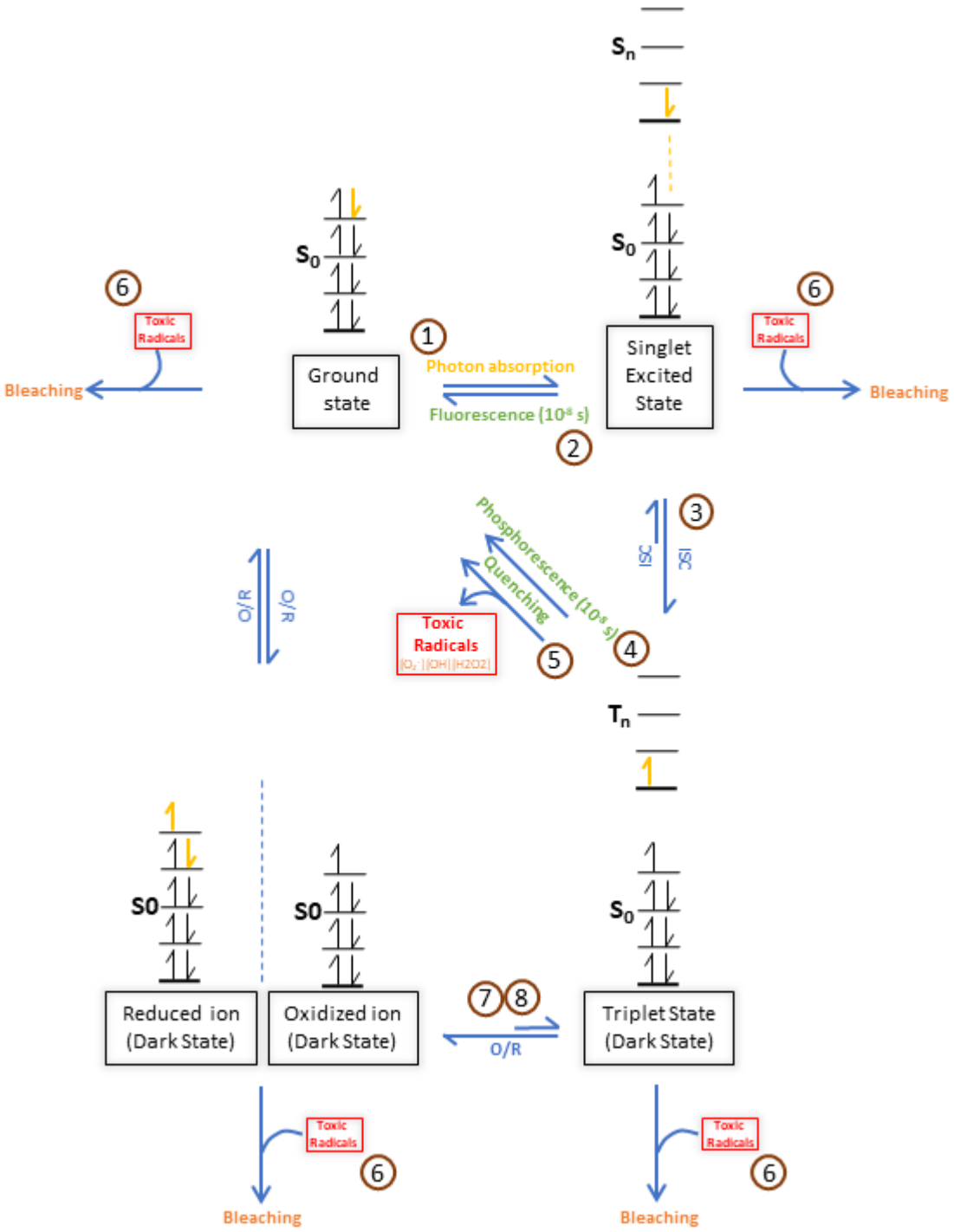

Figure 1.1: Photophysical process of the fluorescence cycle. Schematic of the current understanding of the photophysical process of fluorescence. Phototoxicity is thought to mainly be mediated by reactive oxygen species from this process.

1.2.2 – Fluorophores

A fluorophore is the general term given to any molecule that can absorb light energy and emit that energy in the form of a photon with a longer wavelength and lower energy. In the life sciences, there are two major classes of fluorophores: organic dye molecules and fluorescent proteins. Each of these classes have different properties giving them inherent advantages or disadvantages for certain applications of fluorescent microscopy. However, they are both subjected to the same principles of the photophysical process of fluorescence described in the previous section. Organic fluorescent molecules have a structure built around a conjugated chromophore base that can be conjugated to different molecules or modified with different side chains to confer specificity to certain protein targets or cellular compartments[14]. For example, dyes conjugated to long hydrocarbon chains spontaneously insert themselves into the cellular membrane. Organic fluorophores can usually bind directly on cysteine and amino groups, however, this means they lack strong affinity and specificity to bind a single protein at a time. Organic fluorophores are useful when staining a purified population of proteins, but in whole cell labeling, they need to be coupled with a guiding agent to their specific target. This can be done by attaching dye molecules to highly specific antibodies, but other strategies also make use of synthetic peptide targeting, lipid targeting, or biotinylation. As an exogenous stain, a large portion of organic dye molecules do not bind to their target. Therefore, their staining requires extensive washing steps to remove free dye molecules, reduce nonspecific binding and avoid high background signals. Nevertheless, these small molecules have attractive properties such as their wide spectral range, small size (1 kD), high photostability, brightness and high quantum yield that often make them an ideal choice.

Fluorescent proteins are another class of fluorophores, which were first isolated from living organisms[15]. As genetically encoded vectors, these probes can be directly coupled to a protein or gene of interest and engineered into the genome of a living sample[16]. This gives them an unrivalled specificity compared to other fluorophores, and their 1:1 expression ratio with their tagged gene or protein of interest allows for accurate quantification. Genetic probes don't require exogenous agents or stressful staining procedures, which makes them the probe most suited for live imaging. These fluorescent proteins have a rather large size of 25-30 kD which may sometimes be larger than tagged proteins themselves. Therefore, proper controls must be carried out to ensure tagged proteins retain their biological function and aren't significantly affected by steric hindrance from their associated fluorescent proteins[14]. Nonetheless, genetic probes provide excellent simplicity in experimental applications, and their unparalleled specificity and good contrast makes them a very successful and popular option.

1.3– Photobleaching

1.3.1– Dark state reactions

The dark states of a dye refer to its various reversible conformations during which it cannot emit fluorescence. Dark states are typically undesired because they decrease the fluorescence signal. Interestingly, some applications have harnessed their reversible nature to their advantage. Such is the case in the super resolution Stochastic Optical Reconstruction Microscopy (STORM) technique[17]. In the vast majority of other techniques, however, dark states are dreaded as the precursors to the permanent photobleaching reactions that cause the eventual loss of fluorescence from a specimen through the course of an imaging session. Fluorophores enter the triplet state, the first major dark state, following intersystem crossing from the excited singlet state (Fig. 1.1, Step 3). The triplet state of a fluorophore is temporary, but it is orders of magnitude longer lived (us to ms) than the singlet state (ns) which can result in the buildup of a triplet state population as excitation cycles continue. Since molecules in the triplet state cannot emit fluorescence, they form a bottleneck that can deplete dye molecules from the ground state pool. Consequentially, a lower number of molecules are capable of undergoing the fluorescence excitation-emission cycle which results in an overall considerably reduced florescence emission. This process is particularly problematic with dyes that have a high intersystem crossing quantum yield, as they quickly reach emission saturation where many molecules are trapped in the triplet state.

Furthermore, chemical reactions with neighbouring molecules can proceed from the highly energetic singlet and triplet excited states, though these are only significant from the triplet state because the lifetime of the singlet state is too short (ns) to allow subsequent interactions. Dissolved atmospheric oxygen is a very powerful and ubiquitous oxidiser which tends to be the major reactant and will be considered in this study. The excited triplet state can react with oxygen and harmlessly return to the ground state via two pathways (Fig. 1.1, Step 5). The first pathway is a physical quenching wherein oxygen enhances intersystem crossing, with the end-products being both oxygen and the dye in their respective ground electronic states: $T^* + O_2 \rightleftharpoons S + O_2$ (where T* is the excited triplet state and S is the ground state). The second reaction leads to the quenching of the triplet state as well, however, the end products of that reaction are the ground state and oxygen in its excited singlet state: $T^* + O_2 \rightleftharpoons S + O_2^-$. Oxygen in its singlet state is extremely reactive. This will be discussed in more detail in Section 1.4.2. Singlet oxygen, along with other Reactive Oxygen Species (ROS) can react with dye molecules in their ground and excited states and result in the breakdown of chemical bonds (Fig. 1.1, Step 6) leading to destruction of the molecule and permanent photobleaching[18-20]. Aside from oxygen, another major reactant with the excited triplet state is second fluorophore molecule in the excited state (Fig. 1.1, Step 7 and 8). Dye-Dye reactions can

become dominant in conditions where the concentration of fluorophores is high. Triplet-Triplet, and Triplet-Singlet interactions can yield semi-oxidised and semi-reduced molecular forms, which will be termed radicals or ions hereafter: $T^* + T^* \rightleftharpoons X + R$ and $T^* + S^* \rightleftharpoons X$ (where R is the reduced form, and X is the oxidised form). Radicals are another dark state of dye molecules, as they generally cannot emit fluorescence. The fluorophore's lifetime in the dark state depends on its stability, but further reactions will eventually occur returning the dye to its ground state, or to a permanently bleached yet stable form[21,22]. Another layer of complexity is added to the photophysical processes when multiphoton absorption is considered. Under high incident light power, all molecules can be excited to the single state leading to a situation termed ground state saturation. Under these conditions, the probability of an excited dye molecule absorbing a second or potentially third photon of energy becomes highly favored. This can occur from either the singlet or triplet excited states, which would excite the molecules to higher electronic excited state levels. This is a very problematic occurrence for dye molecules because the higher level excited states are significantly more reactive and more likely to undergo destructive photochemical reactions. These reactions can also open the door to direct ionisation of molecules, as well as higher order reactions and atom rearrangements [23-27].

In summary, two reactions can lead to the bleaching of a fluorophore: (1) ROS attack, and (2) further modification of the radical forms. In principle, there exists an equilibrium between the two mechanisms at a given time depending on the fluorophore, fluorophore concentrations and environmental parameters such as oxygen concentration. However, different mechanisms can dominate depending on experimental conditions. For example, there is strong evidence that at low incident light power, photobleaching from ROS attack is predominant, whereas at high incident light power pathways involving radical forms are more important[18,20,28,29]. For instance, the inefficiency of anoxia at reducing photobleaching at high light powers is likely due to radical forms dominating photobleaching reactions. Dye concentration also plays a strong role in the balance between the two mechanisms. A high dye concentration favors dye-dye reactions in excited forms over diffusion dependent dye-oxygen reactions. As such, dye-dye reactions would be expected to be the main concern when fluorophores are localised and densely associated with their target, whereas the dye-oxygen ROS reactions would be most problematic with diffusing or sparsely localised fluorophore that have little to no contact with neighbouring dye molecules. Overall, these processes are complex as other factors, such as temperature or pH can also influence the equilibrium.

1.3.2– Autofluorescence and radical by-products

The first and most popular fluorescent protein known as green fluorescent protein (GFP), was discovered and first isolated from the *Aequorea victoria* jellyfish by Osamu Shimomura in the early 1960s. GFP has since become the foundation for an entire field of protein engineering that has led to proteins of various colours that are used as exogenous fluorescent markers in thousands of applications[30]. A plethora of other molecules endogenous to cells can also undergo the cycle of fluorescence in addition to external probes and this process is known as autofluorescence. Most of these molecules are not readily detected during fluorescence microscopy imaging because they have low light absorption and dim fluorescence emissions that are insignificant relative to the emission of fluorescent dyes. Nevertheless, autofluorescent molecules can undergo the same photophysical cycle and emit the same by-products as other fluorophores, which can contribute to the overall toxicity exerted during fluorescence microscopy applications. Using conditions that reflect typical widefield fluorescence microscopy, Gorgidze et al. imaged pig kidney embryo cells lacking any fluorescent proteins with blue light (467 nm) and found that cells underwent mitotic arrest after a mere 15 second exposure time[31]. This indicated the presence of phototoxic reactions from native molecules within the cells, which they attributed to autofluorescent granules that were localised on the mitotic spindle. A greater understanding of a variety of specific molecules that can be autofluorescent in nature is being gained. Flavin adenine dinucleotide (FAD) and nicotinamide adenine dinucleotide (NADH) for instance are key molecules in the metabolic machinery of cells, and they each have a chromophore domain that can absorb light at wavelengths of 515 nm and 365 nm, respectively[32]. Autofluorescent molecules can also be found in the live cell imaging media, such as riboflavin (vitamin B2), which has been shown to induce phototoxic effects when present in Dulbecco's Modified Eagle Media (DMEM) cell culture media. Removing riboflavin from the imaging media has been shown to significantly reduce toxic effects seen in oligodendrocyte progenitor cells, which had been attributed to riboflavin autofluorescence induced ROS[33,34]. In light of these studies, it is important to be mindful that molecules other than the intended fluorescent dye can absorb incident light during fluorescence microscopy and contribute to the overall phototoxicity and photobleaching.

1.4 – Phototoxicity

1.4.1 – General light toxicity

Light excitation in fluorescence microscopy exposes a sample to an innumerable quantity of photons. Unfortunately, most photons do not come into contact with a fluorophore molecule, and those energy vectors can result in unintended reaction pathways within a sample. Perhaps the best-known example of light induced toxicity is the mutagenic properties of UV light, that causes tissue damaging sunburns. UV light produces the most energetic type of photons used in fluorescence microscopy, and this high energy light is the most hazardous to cellular health. UV absorption can facilitate photochemical reactions that can result in harmful changes within a cell. In the case of DNA for example, this can lead to mutagenic pyrimidine dimerization[35]. UV light also contains enough energy that can cause direct ionisation of molecules. H_2O molecules, which make up a big portion of cellular content, can be ionised and split to produce hydroxyl (OH^-) radicals that constitute a major toxicity agent when imaging with such wavelengths[36]. Light in the visible wavelengths can also induce cellular damage. For instance, violet and blue light (400-490 nm) have been shown to stimulate H_2O_2 production in peroxisomes and mitochondria which induce cellular stress[37]. Similarly, human primary retinal epithelial cells exposed to visible light (390-550 nm) displayed mitochondrial DNA damage in addition to stimulated singlet oxygen, superoxide anion and hydroxyl radical production[38]. Interestingly, photodamage can also arise from a purely physical source, such as localised heating from focused infrared incident light in the field of view being imaged. Blay and Price showed that cellular function, assayed through mitochondrial activity and DNA fragmentation and synthesis, was inhibited when the temperature moderately rose to 42 ººC from the standard 37 ººC usually implemented during live cell imaging[39]. These problematic events can be expected to arise whenever a sample is exposed to light, in addition to the other toxicities that come into play when fluorophores are present.

1.4.2 – Radical by-products of fluorescence

A radical species can be defined as any molecule that can exist for a given period of time containing one or more unpaired electrons. In fact, atmospheric oxygen (O_2) in its most stable form is a free radical, as it has 2 unpaired electrons making it a powerful oxidant. However, it does not interact readily with stable molecules because both its single electrons have the same electronic spin. Therefore, it would require 2 other electrons with the same spin opposite to its own to fill the vacant positions it has. A pair of electrons in an atomic orbital of a stable molecule cannot satisfy this requirement as they have opposing spins ($+\frac{1}{2}$ and $-\frac{1}{2}$), which inhibits oxidation by oxygen. However, this is not the case with radical

molecules, such as ionic forms or radicals with which O_2 reacts swiftly through single electron transfer reactions. Energy absorption by an O_2 molecule can reverse the spin of one of its reactive electrons which transfers the molecule into its singlet electronic conformation. This dramatically increases its reactivity as it removes the spin restriction and enables the radical to directly oxidise stable molecules such as proteins, DNA and lipids. If the singlet oxygen acquires an electron into one of its two vacant positions, it becomes the superoxide radical anion. Left with only 1 empty electron orbital, this radical remains largely reactive. A variety of other reactions can yield yet more forms of radical oxygen species which encompasses a plethora of additional oxygen construct including reactive chlorine species, reactive bromine species, and reactive nitrogen species[36].

ROS involved in the bleaching of dye molecules can be equally associated with the phototoxicity observed in fluorescence microscopy. While the exact mechanisms have yet to be described, it is thought that the singlet oxygen species is the main ROS product of the fluorescence process[7]. But as described before, singlet oxygen radicals can lead to the formation of an array of further radicals. One of the ways in which radicals can exert their toxicity is by (1) combining with other molecules[36]. For instance, addition of the hydroxyl radical (OH) to the 8^{th} ring position of the guanine nucleic acid base can prime the base for mutagenic oxidation reactions. Radicals can act as (2) oxidising or (3) reducing agents, catalysing the formation of more complex radicals and reactive ions of otherwise stable molecules. Radicals may also (4) cleave hydrogen atoms from other molecules. An example is seen in the hydrocarbon side chains of polyunsaturated fatty acid residues in cellular and organelle membranes, where removing a hydrogen atom opens the negatively charged carbon to react with O_2, forming peroxyl radicals. These go on to oxidize membrane proteins and take hydrogen atoms from neighbouring hydrocarbon side chains, leading to the formation of new peroxyl radicals and themselves becoming peroxide molecules. Evidently, this triggers a chain reaction that propagates from one hydrocarbon to another. This peroxidation is further aggravated by the ability of singlet oxygen to directly react with hydrocarbon side chains on different carbon positions leading to the formation of a variety of peroxide species. Eventually, peroxidation of the lipid bilayer decreases its fluidity and increases its permeability. Consequently, the leaky membrane allows substances that are usually blocked or controlled through channels to pass, while membrane associated proteins, enzymes and channels become non-functional. Eventually, membrane integrity is lost and organelles, such as lysosomes, can rupture and release their own toxic reactants which ultimately lead to cellular death.

An example of ROS toxicity is seen in Dixit and Cyr's study where they showed that tobacco BY-2 cells underwent increased mitotic arrest when subjected to high levels of excitation light[40]. This increase was correlated to the increased concentration of ROS within cells. Another example of ROS mediated phototoxicity can be seen with the autofluorescent molecules NADH and FAD, which are commonly used as indicators in oxidative energy metabolism studies[32]. As FAD undergoes the fluorescence cycle it can generate ROS, and the FAD population consequentially undergoes decomposition. FAD depletion can severely affect cellular viability as this molecule is intricately involved in the metabolic system. Breakdown of NADH in a similar manner is even more problematic as the molecule is also involved in a multitude of cytosolic and mitochondrial reactions and compromising the NADH population or even it's redox balance can hold a wide range of consequences across a cell. ROS originating from exogenous fluorophores can also disturb FAD and NADH populations and inhibit their crucial biological function, therefore it is necessary to implement solutions to limit phototoxicity in fluorescence microscopy.

1.5 – Limiting photodamage

1.5.1 – Quenching of the dark states

The study the fluorescence process and its photophysical apparatus can lead to understanding key steps that can be targeted to limit harmful interactions. Perhaps the most obvious step is to quench the triplet state, being the precursor of most light induced toxicity. Although toxic reactions can theoretically proceed from the singlet excited state of a dye, the lifetime of this state is physically too short for any significant chemical reaction to proceed. Triplet states on the other hand have relatively long lifetimes and removing them would, in principle, remove much of the phototoxicity and photobleaching. An elegant parallel of such a manipulation can be drawn from the process of photosynthesis in plants[36]. Insufficient energy dissipation during photosynthesis can lead to the formation of a significant population of chlorophyll molecules in the triplet state. The reactive triplet state chlorophyll molecules can then transfer their energy to neighbouring O_2 molecules and produce singlet oxygen radicals that can in turn oxidise chloroplast molecules and trigger phototoxicity in cells. To counter this, plants use pigment molecules called carotenoids to directly quench both the triplet chlorophyll and the singlet oxygen molecular states. In fluorescence imaging, other problematic states are the radical forms of the dye that are important precursors to photodamaging reactions[7,11]. Photodamage is generally generated through a variety of reactions incurred from the triplet, oxidised

and reduced forms of a fluorophore. Therefore, while the triplet state should be the main target of quenching, a better solution would rely on the quenching of all the dark states.

Mercaptoethylamine (MEA) is an example of a reagent that has been shown to not only be an effective triplet state quencher, but also an ionic form quencher[41]. In their study, Song et al. flushed out oxygen from an imaging plate using argon, an inert noble gas. They then added MEA in successive concentrations, and found that increasing concentrations effectively reduced the triplet, semi-oxidised and semi-reduced forms of the fluorescein and eosin dyes. Due to the fact that oxygen was absent in the system, the reduction was attributed to quenching mediated by MEA. One limitation of this reagent is that oxygen can act as a reducing agent, meaning that in typical imaging settings with oxygen present MEA can readily react with it. This results in an interesting dynamic of competing reactions between Dye-Oxygen, Dye-MEA, and Oxygen-MEA. However, oxygen levels generally subside after some time from MEA addition. Given adequate MEA concentrations, the main reactions then become between the dark states and MEA which results in their efficient quenching.

Moreover, elaborate solutions can be developed if redox chemistry is exploited. For instance, the triplet state population can be induced to react with a reducing agent to transfer it into the reduced form of the dye. The reduced form can subsequently react with an oxidising agent to return to the ground state. The reverse reaction where an oxidising agent is first used followed by a reducing agent is also true. Evidently, this would require both the oxidising and reducing agents not to be excessively reactive so as not to react with each other instead of the triplet state dye. The combination of ascorbic acid and methyl viologen has been shown to work well in this manner[10]. Another reagent that fulfills this need is Trolox (Hoffmann-La Roche Inc.) which is unique in that it fulfills the role of both the reducing and oxidising agents at the same time. This is because some of the Trolox population will degrade as it is dissolved in solution, forming a quinone derivative. This Trolox-quinone product is an oxidant, whereas the original Trolox molecule is a reductant, making Trolox a convenient reagent to apply[42].

1.5.2 – Scavenging of oxygen in solution

Oxygen is ubiquitous within the imaging media and a sample. One method of preventing oxygen from reacting with the triplet state and the ionic forms of a dye is to simply remove it from the imaging environment. A commonly used system is the combination of glucose oxidase and catalase enzymes, which oxidise glucose and thus deplete it from solution. The issue with this method is that the by-product is gluconic acid, which results in considerable acidification of the cellular environment[43]. Another oxygen scavenging system is the protocatechuic acid (PCA)/protocatechute-3,4-dioxygenase

(PCD) enzyme combination. The PCD enzyme catalyses the conversion of PCA to β-carboxy-*cis, cis*-muconic acid, which consumes oxygen in the process[44]. However, a significant issue arises in the depletion of oxygen: unless an anaerobic organism is being imaged, the sample needs oxygen for physiological functions. From a purely metabolic approach, cells can rely on glycolysis for energy production, relinquishing the need for oxygen for a period of time, which seems to be the case in culture conditions where glucose is readily available[45]. However, removing oxygen from solution would effectively shut down oxidative phosphorylation, as well as all other processes using oxygen which may in itself stress the cell or result in serious misrepresentation of physiological conditions.

Another valuable approach would be to eliminate ROS as they are produced which would prevent their damaging reactions. In fact, most cell types already have intrinsic mechanisms to quench ROS, however, inducing ROS production quickly overwhelms cellular mechanisms and causes extensive toxicity. Unfortunately, there are complications associated with selectively quenching ROS. These molecules are extremely reactive and tend to react with molecules in their immediate environment. This means any product that would target them needs to be present in high concentrations within a cell, which in itself may be problematic to cellular health. Additionally, there is not a single product that can target all ROS at the same time, meaning there would need to be many exogenous agents in the cellular environment to efficiently reduce toxicity, and compensating for their subsequent reactions would be difficult. Nevertheless, such reagents include sodium pyruvate supplements which can target hydrogen peroxide, mannitol which targets hydroxyl radicals, and sodium azide that targets singlet oxygen. Alternatively, antioxidants can be supplemented into the growth media to enrich cellular environments and provide them with an innate level of protection again ROS[46].

1.5.3 – Choice of imaging dye

There is a vast selection of fluorophores in both organic dyes and proteins that are available in a diverse assortment of excitation-emission spectrums. There are many dyes on the market that are considered popular in fluorescence microscopy, however researchers should consistently explore their range of options in a field that is constantly evolving. There are key characteristics that constitute an ideal fluorophore in regard to their vulnerability to photodamage[47]. The extinction coefficient of a dye is a measure of how efficiently it absorbs light. A good extinction coefficient indicates a smaller number of photon input is needed to excite a given number of molecules. Another important characteristic is the quantum yield, which is the ratio of the number of photons released versus photons absorbed. The closer that ratio is to 1, the better, as it indicates radiation efficiency, and again less light is required to

achieve the same amount of signal output. Brightness of a dye is therefore a combination of these two metrics. Photostability of a dye should also be considered, which is a measure of the number of excitation/emissions cycles a molecule can undergo before photobleaching. Some molecules are intrinsically more resistant to photo- and environment-induced bleaching, making them a more suitable choice for long term imaging.

Finally, the excitation spectrum of a fluorophore should also be seriously considered. As was discussed in Section 1.4.1, light can inflict collateral damage on biological functions. Studies have consistently shown that the color of light being delivered to the sample can make a difference as to the generated phototoxicity[31,46,48-50]. Waldchen et al. for example, imaged cells using a 488 nm laser with a given light intensity and noted they all died. They then imaged another set of cells with the same light intensity but using the less energetic 514 nm laser and observed that all cells had survived. In a subsequent experiment, they used a light intensity at which all cells died using the 514 nm laser and imaged another set of cells with the same light intensity but with the 558 nm and 640 nm laser wavelengths. Cells survived at rates of 85% and 100% with the 558 nm and 640 nm wavelengths, respectively. This demonstrates how sensitive cells can be to the energy level of the light illuminating them, and how important it is to choose red shifted dyes whenever possible when doing fluorescence imaging. While implementation of these dyes is valuable, the major limitation when using red dyes is the reduced resolution red wavelengths provide compared to shorter wavelength alternatives. However, many applications will not require high enough resolution for this to be an issue[48].

1.6 – Objective, hypothesis and rational

Photodamage is a common issue encountered in fluorescence microscopy-based techniques, unfortunately, this issue has been consistently overlooked by researchers. Too often are proper controls not applied to detect phototoxicity, and this could possibly lead to erroneous or clouded conclusions[51,52]. The methods summarised in Section 1.5 are potential solutions, however they can considerably alter the physiological environment of a sample, which in itself may induce stress and affect experimental results. Furthermore, these alternative systems may also be incompatible or perturb biological systems[53]. Many of these reagents, including the oxygen scavenger PCA and the dark state scavenger Trolox, have been shown to modify the cellular membrane bilayer properties to varying degrees[54]. Therefore, there is still a need to find less invasive solutions to reduce phototoxicity, which has been the objective of this thesis.

It is common knowledge amongst microscopy users that exposing a fluorescent sample to light for an extended period of time could result in unfavorable conditions, particularly photobleaching the dyes. This issue is rationally addressed by minimizing the exposure of a sample to light which effectively reduces the excitation/emission cycles a fluorophore undergoes and therefore reduces the downstream probabilities of unwanted reactions from occurring. However, using a low exposure time results in a poor signal yield, and poor experimental data. This compels users to accordingly increase the excitation light power to generate acceptable fluorescence images. This study argues that this is not the best approach to maximise the lifetime of an imaging specimen, both in terms of its physiological health and the rate of bleaching it undergoes. The hypothesis is that in order to increase signal yield, the light power should be kept at a low intensity, and the exposure time of a sample should be increased until an acceptable signal is reached. This counterintuitive approach is justified based on the current understanding of the photophysical apparatus of the fluorescence process. Fluorescence signal yield is dependent on the amount of productive excitation-emission cycles a given population of fluorophores collectively undergo. Higher light powers, or a higher flux of photons increase the population of excited fluorophores in a given time and consequently the fluorescence signal is increased. Alternatively, a low light power coupled with a long exposure time can yield the same number of excitation-emission cycles. In practice, cameras integrate signal over a given exposure time and therefore the final images obtained using either methods would be essentially equivalent. However, this study argues that increasing the exposure time, rather than power results in a significant reduction of photodamage because there are fewer dye molecules in the triplet state at all times. This reduced triplet population, along with the reduced photon density in low light powers dramatically reduces undesired multiphoton excitation events[25,55].

Furthermore, light emission has traditionally been implemented as a constant, steady release of photons from a light source. Common incandescent lamps function by passing electricity through their metallic filament, which increases the temperature and subsequently emits light from the filament. The more intense mercury arc lamps used in fluorescent microscopy emit a constant stream of photons in a spectrum spanning the UV to the IR as mercury droplets are vaporised and ionised. The onset of the new, more efficient and competitive light sources called light emitting diodes (LED) have changed the dynamics of how light is delivered as they can quickly be turned on and off. This was instrumental at saving lamp usage time and energy consumption, however, this also revealed an entirely new application for light sources: pulsed illumination. The light can be rapidly shuttered off and on using electronics allowing for light to be delivered in discrete intervals. During this time the camera collects

the light over an extended exposure time that encompasses these small emissions of light from the excitation cycles in the sample. This study hypothesised that given the same total number of photons per image, delivering the light using square wave pulses would result in reduced levels of photodamage. This is rationalised by the fact that during the rest times between each pulse cycle, much of the dark state population will have time to relax back to the ground state before the next pulse. This results in controlling the overall population of dark state molecules which decreases their availability to react with oxygen and ROS, as well as the probability of double photon absorption events from occurring. Similarly, because only a small population of fluorophores are excited during each pulse, the frequency of transition into the triplet state is dramatically reduced compared to non-pulsed illumination. This in turn reduces the probability of harmful downstream reactions from materialising.

Chapter 2

Materials and Methods

2.1 – Cell culture techniques

2.1.1 – Cell growth and transfection

Chinese hamster ovary K1 (CHO-K1) cells (Cat. no.: 85050302, Sigma Aldrich) were grown in low glucose (1.0 g/L) Dulbecco's Modified Eagle Medium containing L-glutamine, 110 mg/L sodium pyruvate and pyridoxine hydrochloride (Cat. no.: 11885-084; Thermo Fisher Scientific). The media was supplemented with 10% vol/vol fetal bovine serum (Cat. no.: 10082-147, Thermo Fisher Scientific), 1% vol/vol 100x non-essential amino acids (Cat. no.: 11140-050, Thermo Fisher Scientific), 25 mM of 4-(2-hydroxyethyl)-1-piperazineethanesulfonic acid (Cat. no.: 15630-080, Thermo Fisher Scientific), and 10000 units per mL penicillin-streptomycin (Cat. no.: 10378-016, Thermo Fisher Scientific). CHO-K1 cells stably expressing paxillin-EGFP were obtained from the lab of Dr. Rick Horwitz (University of Virginia, Charlottesville, VA), and they were maintained with an addition of 0.5 mg/mL of geneticin (Cat. no.: 10-131-027, Thermo Fisher Scientific) antibiotic for selection of paxillin-EGFP expressing cells.

Transient transfections were performed using the manufacturer protocol for the Lipofectamine 2000 transfection reagent (Cat. no.: 11668-027, Thermo Fisher Scientific). Cells were grown to 70-85% confluence in 6 well tissue culture plates. Aliquots of 1 μg of DNA construct and 2.5 μL of Lipofectamine 2000 were diluted into separate Eppendorf tubes in phenol red free optiMEM media (Cat. no.: 11058-021, Thermo Fisher Scientific) to a total volume of 150 μL. The solutions were left for 5 minutes at room temperature, after which they were combined into 1 tube, then mixed and incubated at room temperature for 20 minutes to allow DNA-liposome encapsulation. The DNA-Lipofectamine solution was then diluted with 1.7 mL optiMEM to a final volume of 2 mL and added to designated wells containing cells in the 6-well plate. Finally, cells were incubated with the transfection solution for 5-6 hours, after which it was replaced with full growth media with antibiotic selection. The DNA plasmid construct used, mCherry-paxillin, and cells stably expressing Paxillin-EGFP were a gift from the lab of Dr. Rick Horwitz (University of Virginia, Charlottesville, VA).

2.1.2 – Imaging plate preparation

Imaging was performed in 35-mm glass bottom plates (Cat. no.: FD-35, World Precision Instruments). Plates were coated with 2 mL of a 2 μg/mL solution of fibronectin (Cat. no.: F-0895, Sigma Aldrich) in warm Phosphate Buffered Saline (PBS) at 37^{o}C under 5% CO2 for 1 hour. Surfaces were

subsequently washed with PBS twice, then either immediately used or stored at 4°C while immersed in 1mL PBS for up to a week.

Prior to plating, cells were grown to 70-85% confluence. Growth media was aspirated and 1 PBS wash was performed. Cells were then lifted by incubating them at 37°C for 4 minutes in trypsin/EDTA solution (Cat. no.: 25200-056, Thermo Fisher Scientific). Cells were resuspended in growth media, then plated to ~15% confluency onto fibronectin coated plates. Cells were incubated overnight before imaging. Imaging sample plates intended for the photobleaching assay were fixed by washing cells with PBS three times, followed by application of a 4% Paraformaldehyde solution (Cat. no.: 50-00-0, Polysciences) for 15 minutes. Finally, plates were washed 2 times with PBS, then mounted in 1 mL of PBS.

2.1.3 – Reagents, dyes and staining

Staining of cellular components using organic dyes were performed using the manufacturer protocols. Imaging plates were prepared as before. For Mitotracker Red™ CMXRos (Cat. no.: M7512, Thermo Fisher Scientific), the stock reagent was diluted from 1 mM to 150 µM into 2 mL of warm growth media. The solution was then gently vortexed for 10 seconds. Growth media was removed and the staining solution was added and cells were incubated at 37°C for 1 hour. The dye solution was discarded and replaced with fresh growth media and plates were ready for live cell imaging. Lysotracker Red™ DND-99 (Cat. no.: L7528, Thermo Fisher Scientific) staining was done using a similar procedure, though the working concentration was 50 nM. For the photobleaching assay, fixation was done as above. However, Mitotracker Red™ samples had to be left for at least 5h at 37°C to enhance retention of the dye to the mitochondria.

ProLong Live™ (Cat. no.: P36974, Thermo Fisher Scientific) was a singlet oxygen scavenger system used in this study. Stock reagent was diluted 1:100 by adding 20 µL to 2 mL of warm growth media. The solution was mixed then added to the imaging plate. Cells were incubated at 37°C for at least 15 minutes before imaging, and the reagent was kept in solution throughout experiments.

2.2 – Microscopy

2.2.1 – Imaging

Light Power Variation Experiments. Widefield microscopy experiments were performed on a Zeiss AxioObserver fully automated inverted microscope (Carl Zeiss, Jena, Germany). Cell migration and protrusion assays were conducted with a 20x Plan-Apochromat/0.8 NA objective lens and photobleaching experiments with a 63x Plan-Apochromat/1.4 NA oil immersion objective lens. Fluorescence incident light

was provided by an X-cite 120LED (Fig. 2.1A) white light source (Excelitas, Waltham, MA). Power intensity was measured at the beginning of each experiment with a 10x Plan Neofluar/0.3 NA objective lens using an X-cite optical power measurement meter (Excelitas, Waltham, MA). Filter cubes were selected to match the excitation-emission spectra of each dye: filter set 10 (Fig. 2.1B) for EGFP, and filter set 71 (Fig. 2.1C) for mCherry and MitoTracker Red™ (Carl Zeiss). Experiments were performed using the LED light source TTL electronic shutter directly coupled to the system's Hamamatsu Orca ER camera (Hamamatsu, Hamamatsu, Japan) to control the exposure time at a high level of accuracy. Confocal microscopy experiments were performed on a Nikon A1R fully automated inverted microscope (Nikon, Tokyo, Japan). Cell protrusion assays were performed with a 20x Plan-Apochromat/0.75 NA objective lens and photobleaching experiment with a 60x Apochromat/1.4 NA oil immersion objective lens. Laser power was measured from a 10x plan-Apochromat/0.45 NA objective lens. For the photobleaching experiments, fixed cells were stored at 4°C and used over a period of 4-6 weeks with no visible signs of deterioration. Images were sequentially acquired on the microscope until fluorescence intensity decreased to a plateau and photobleaching ceased. For live cell experiments, cells were mounted in 2 mL of growth media, with additional reagents when appropriate. They were kept at physiological environmental conditions using a top-stage incubator system (Live Cell Instrument, Seoul, Korea). Cells were imaged for every 2 minutes for 4-6 hours for cell migration assays and every 20 seconds for 30 minutes for the cell protrusion assay. In all cases, light power and exposure time were set according to the settings listed in tables 3.1 and 3.2.

Light Pulsing Technique. Experiments were performed on a Zeiss AxioObserver fully automated inverted microscope coupled with a Hamamatsu Orca-ER camera (Hamamatsu). Cell protrusion assays were performed with a 20x LD Plan/0.35 NA objective lens and photobleaching experiments with a 63x Plan-Apochromat/1.4 NA oil immersion objective lens. Fluorescence incident light was from a pE-4000 light source (CoolLED, Andover, UK). The unit combines a set of 16 different colored LEDs to produce light across the visible spectrum (Fig. 2.1A). The option to activate single LEDs one at a time was used in this study. The 470 nm LED was used to excite EGFP and the 580 nm LED for mCherry and MitoTracker Red™. LED output power was measured at the beginning of each experiment with a 10x EC-Plan-Neofluar/0.3 NA objective lens using an X-cite optical power measurement meter (Excelitas). Filter cubes were selected to match the excitation-emission spectra of each dye: filter set 49011 (Fig. 2.1D) for EGFP (Chroma Technologies Inc., Bellows Falls, VT), and filter set 71 (Fig. 2.1C) for mCherry and MitoTracker Red™ (Carl Zeiss). Pulsing functions were triggered using the light source's integrated function generator, which

enabled various customisation options including the pulse amplitude, period and duty cycle. Photobleaching and protrusion assays were performed as described above. The light power, exposure time, and pulsing settings used in each experimental set are listed in Tables 4.1, 4.2, and 4.3.

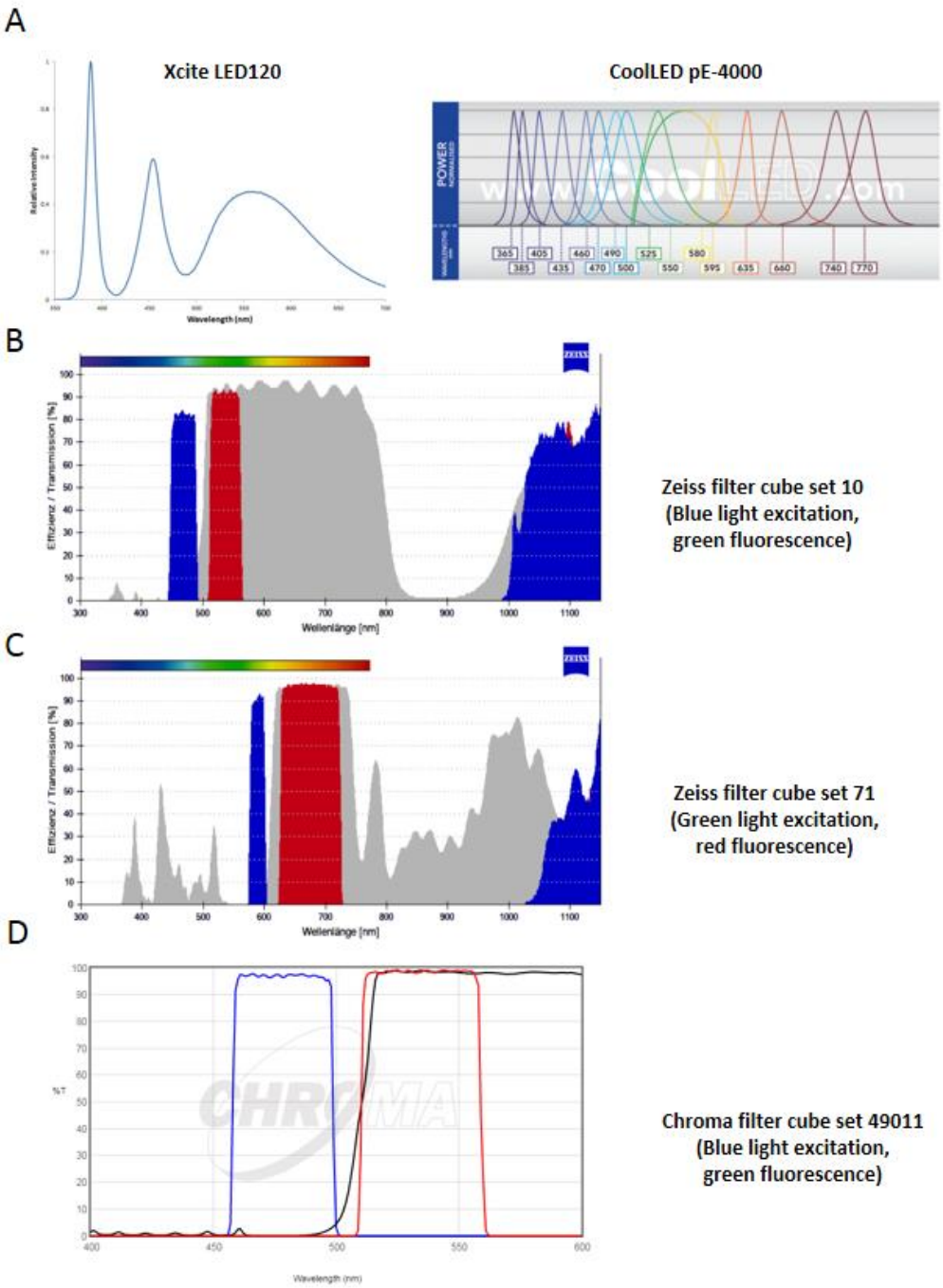

Figure 2.1: Spectral profile of LED light sources and filter cubes used throughout the study. (A) Relative intensity of the Xcite LED120 LED in the ultra violet-visible-infrared wavelength spectrum. (B) Relative intensity of the CoolLED pE-4000 LED in the ultra violet-visible-infrared wavelength spectrum. (C) Transmission % of the Zeiss filter set 10. The blue outline highlights the excitation spectrum, the red outline highlights the emission spectrum, and the gray outline highlights the dichroic. (D) Transmission % of the Zeiss filter set 71. (E) Transmission % of the Chroma filter set 49011.

Setting Pulsing Function in Light Source Generator. Several customisations are available in the LED function generator of the pE-4000 light source. In this study, the pulse amplitude, period duration and duty cycle were used. The amplitude corresponds to the light power, which varied according to experimental conditions. Pulse period is the duration of a pulse, in addition to its associated down time (off, or rest period). The duty cycle dictates the percent (%) of the pulse period duration during which light output is turned on. For example, given a period of 125 µs with a duty cycle of 20%, the corresponding pulse width would then be 25 µs with 100 µs rest time. All duty cycles used in Chapter 4 are listed below.

Table 2.1: LED function settings for square pulses. Orange are settings corresponding to Table 4.1; blue are for Table 4.2; yellow are for Table 4.3.

	1	2	3	4	5	6	7	8	9	10	11	12
PULSE WIDTH (µS)	34	59	109	109	109	109	109	109	109	59	109	159
REST TIME (µS)	100	100	100	25	50	100	150	200	300	50	100	150
PERIOD (µS)	134	159	209	134	159	209	259	309	409	109	209	309
DUTY CYCLE (%)	25	37	52	81	69	52	42	35	27	54	52	52

2.2.2 – Analysis

Analysis of cell migration. Cells were manually tracked in MetaXpress analysis software (Molecular Devices). X, Y position data for each cell track were then exported to MATLAB (v. 8.6, Rel. R2015b; The MathWorks). Rose plots of cell movement were created by superimposing the starting position of each track on the origin (0,0). The average speed of each 10-minute segment was then calculated by determining the mean distance travelled between each time point over the imaging interval. The average speed of each cell was calculated in a similar fashion. The data shown represents the mean ± standard error of the mean (s.e.m.) for all cells analyzed from three independent experiments. The MatLab script for this was written by Alexander Kiepas (Claire Brown Lab, McGill, Qc).

Analysis of cell protrusion assays. CHO-K1 cells were seeded onto 35-mm dishes and imaged every 20 seconds for 30 minutes, as described above. Incident light powers of 23 mW, 12 mW, 6.7 mW and 1.6 mW were coupled to exposure times of 24 ms, 47 ms, 84 ms, and 350 ms, respectively. Image

stacks were analyzed in MetaXpress using the kymograph function. The kymograph generates a graph of membrane displacement versus time, in which the slope represents the speed of protrusion. The data shown represents the mean ± s.e.m. for all cells analyzed from three independent experiments.

Analysis of cell photobleaching assay. The fluorescence intensity was measured within multiple 100x100 pixel regions of cells over the image stack, and the data for each region was fit to a single exponential decay using Origin (Pro) 9.3 software (OriginLab Corporation, Northampton, MA) with the following equation:

$$y = y_0 + A_e^{-x/t} \quad (1)$$

Where y_0 is the offset value, A is the amplitude and t is the time constant. The halftime of exponential decay (tau) is given by the following equation:

$$tau = t_1 * \ln(2) \quad (2)$$

Each imaging setting was repeated three times with three different experimental preparations of fixed cells. Seven regions of interest (ROI) were selected from at least 3 cells per trial, amounting to 21 ROI per setting.

Statistical analyses. Statistical significance values (*P*-values) for cell migration, protrusion and photobleaching rates were obtained by performing a two tailed *t*-test.

2.2.3 – Calculations

Calculation of the estimated photon count per frame to equalize all power settings. Different imaging conditions can be comparable only if an equivalent amount of light is delivered to the samples during the acquisition of one image. This was achieved by maintaining an equal number of photons delivered per image collected for the different settings. Light power was used to determine the density of photons, which was then used to calculate the appropriate exposure time to equalize settings with different light powers. An example of this calculation is shown below for setting #2 in Table 3.1:

The energy (e) of one photon is given by the equation:

$$e = \frac{hc}{\lambda} \quad (3)$$

where h is Planck's constant (6.626×10^{-34} J • s), c is the speed of light (3×10^{8} m/s) and λ is the wavelength of the photon, which is 488 nm for EGFP excitation. It should be noted that with white LED light sources, filter cubes are used to restrict incident light to a range of photon wavelengths. However, using 488 nm as an estimate across all settings should provide a relative measure of photons for each setting.

Power can be defined as the amount of energy delivered per second and can also be defined as:

$$W = (\text{number of photons delivered per second (n)}) * (\text{energy of 1 photon (e)}) \quad (4)$$

In the above equation, W is the power in watts and n is the number of photons delivered per second. In this example, power was set to be 0.023 W and as such, the number of photons delivered per second was determined to be 5.6473×10^{16} Photons/s.

Finally, the number of photons per second was scaled to determine the number of photons per image for each exposure time:

$$N = n * \text{exposure time} \quad (5)$$

Where N is the number of photons per image. With an exposure time of 0.02435 seconds, the number of photons was determined to be 1.37512×10^{15}. This calculation was then applied to each setting in Tables 3.1 and 3.2.

Equalizing illumination conditions with different pulsing settings by equalizing the total time under illumination.

An exposure time is defined as the time period during which a sample is exposed to a constant stream of light. Introducing pulsing cycles into a light stream essentially breaks it down to small packets. Therefore, if these small packets are added back together, then they should be equivalent in time and they should be equal to the original, non-pulsed exposure time for 2 settings to be equivalent (Figure 2.2).

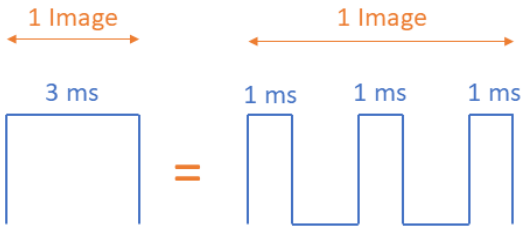

Figure 2.2: Diagram of equivalency between continuous illumination and pulsed illumination.

With this approach, the total number of pulsing cycles by which the original exposure time is broken down into can be determined:

$$\text{Number of cycles} = \text{Original exposure/pulse width} \quad (6)$$

The exposure time of one cycle is composed of an ON pulse width time and an OFF rest time before the commencement of the next cycle. The total exposure time for the acquisition period is then as follows:

$$\text{Total exposure time} = \text{number of cycles x exposure time one cycle} \quad (7)$$

For example, a setting from Figure 4.1 with a power of 22 mW, a non-pulsed exposure time of 25.57 ms, pulse width of 25 µs and a rest time of 100 µs between each pulse will then have a total of 1022. 8 pulsing cycles from equation 6 and a total exposure time of 127. 9 ms from equation 7.

It should be noted that the pulse generator feature is not perfect and inherent delays in electronic signal delivery is present. This has to be accounted for in order to minimize error and increase experimental accuracy. Figure 2.3 shows a graphical representation of the assigned pulsed function (solid blue line) compared to the output from the LED (doted yellow line). Figure 2.4 shows an example of a measurement of a pulse from the 470 nm LED from the pE-4000 light source using an oscilloscope.

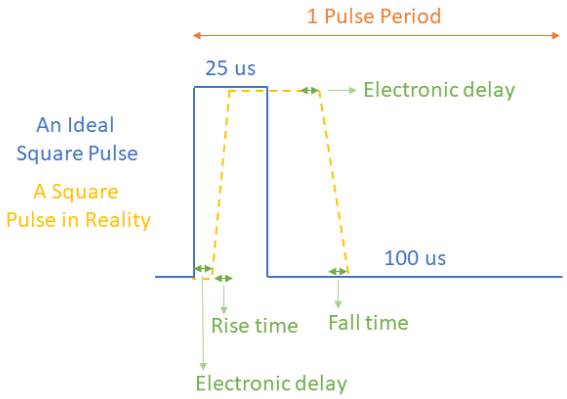

Figure 2.3: Graphical representation of the difference between a theoretical (solid blue line) and a practical square pulse (dotted yellow line).

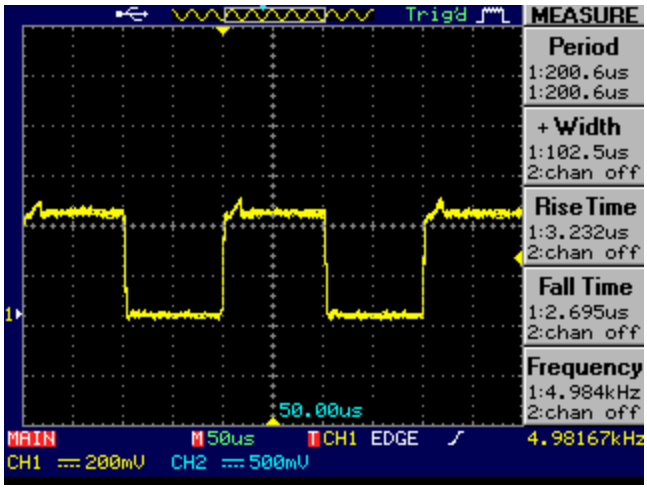

Figure 2.4: Sample oscilloscope measurement of a pulse from the pE-4000 light source, set with a width of 100 µs and a rest time of 100 µs (provided by CoolLED™).

CoolLED (manufacturer) provided the LED response time for electronic delay in triggering the LED to turn on as 14.2 µs. Once initiated, the LED requires a rise time of 1.9 µs to reach its intended power output level. An electronic delay of 5 µs then follow the triggering of the LED to shut down, after which the LED dims with a fall time of 3.5 µs before shutting down. From this information, corrections were determined:

- The electronic delay time in triggering the LED on and off results in a net loss of 9.2 µs to the pulse width time. This lost time is additive. The rest time between pulses and likewise the period of one pulse cycle was thus increased.
- The rise and fall time of the LED resulted in a net gain of 1.6 µs in pulse width. However, the actual loss in light output was much lower than 1.6 µs as light is not at peak power during the rise and fall time.
- Taken together, an estimated 9 µs of LED pulse width needed to be added to each pulse to account for lost light output due to electronic delay and LED response time.

In the previous example shown from Figure 4.1 with an original pulse width of 25 µs and rest time of 100 µs, these values are corrected to 34 µs and 109 µs, respectfully. Given 1022. 8 pulsing cycles obtained from equation 6, and an updated period of 143 µs per pulse cycle, the exposure time for one image was determined to be 146 ms from Equation 7. This calculation was applied to each setting in Tables 4.1, 4.2, and 4.3.

Calculation of estimated photon count per frame light exposure to confirm equivalency between pulsing settings.

Another approach to verify equivalency between light pulsing settings is by maintaining an equal number of photons delivered per image. The number of photons delivered per second (n) can be calculated from Equations 3, 4, and then 5. This number can then be scaled down to determine the photon count per pulse cycle (C) as follows:

$$C = n * \text{time of 1 pulse} \tag{8}$$

The total number of pulsing cycles can be determined using Equation 6. Therefore, the total photon count per image (N) for a pulsing setting can be determined as follows:

$$N = C * \text{number of pulsing cycles per image} \tag{9}$$

Given the same example from Figure 4.1 as before, with a power of 22 mW, a non-pulsed exposure time of 26 ms, pulse width of 25 µs and a rest time of 100 µs between each pulse will then have a total photon count of 1.3×10^{12} per pulse from Equation 8 and 1.3×10^{15} per image from Equation 9. This calculation has been applied to each setting in Tables 4.1, 4.2, and 4.3 to ensure they all deliver an equivalent number of photons.

Chapter 3

Results: Light Power and Phototoxicity

3.1 – Low incident light power and long camera exposure times decrease photobleaching

The hypothesis investigated in this section was that light power is the primary factor affecting the level of photobleaching a specimen undergoes. Four fluorescence microscopy imaging conditions were designed to test this hypothesis and were compared to brightfield imaging (Table 3.1). The first two settings reflected typical imaging conditions employed in fluorescence microscopy experiments with higher light powers of 23 mW (20% light source output) and 12 mW (10% light source output) coupled with shorter exposure times of 24 ms and 47 ms, respectively. In contrast, the other two settings featured lower light powers of 6.7 (5% light source output) mW and 1.6 mW (1% light source output) coupled with longer exposure times of 84 ms and 350 ms, respectively. These settings all delivered a comparable number of photons to the sample during each image acquisition (see Methods Section 2.2.3, Table 3.1). Since the total amount of light per image was kept constant, the image quality was essentially identical with all of these settings (Fig. 3.1A). The photobleaching curves produced when samples of these cells were successively imaged using a 63X/1.4 NA oil immersion objective lens on the other hand were very different. The photobleaching curves of the higher power settings demonstrated a fast, exponential intensity decay as opposed to the slower intensity decay observed when low light powers were used (Fig 3.1B). The photobleaching rates were quantified by fitting to a single exponential decay and taking the frame number and time for photobleaching of half-time of the initial fluorescence intensity. The halftime of photobleaching increased from 620 image frames (1.5 minutes) with the 23 mW power setting to 2376 frames (21 minutes) with the 1.6 mW light setting. This represented a nearly 4-fold reduction in the rate of photobleaching (Fig. 3.1C). Intermediate settings of 12 mW and 6.7 mW fit the same trend with halftime photobleaching rates of 1054 (3 minutes) and 1546 frames (6.5 minutes), respectively. The general applicability of this concept to other fluorophores was tested with CHO-K1-paxillin-mCherry expressing cells. As with EGFP, using lower light powers greatly reduced photobleaching rates compared with higher powers (Fig. 3.1D). These findings suggest that some higher order photobleaching reactions might only occur at elevated light powers and accelerate the overall photobleaching rates. These reactions are likely insignificant (i.e. have very low probability) at low light powers.

	Illumination Setting				
	#1	#2	#3	#4	#5
Light Power (mW)	Brightfield	23	12	6.7	1.6
Exposure Time (ms)	6 ms	24	47	84	350

Table 3.1: Illumination conditions with scaled light powers. Illumination conditions were designed with different light powers, and exposure times were scaled for all settings to deliver a set number of 1.38 x 10^{15} photons per image for cells expressing EGFP, and 1.63 x 10^{15} for cells expressing mCherry (see Chapter 2.2.3). Epi-fluorescence illumination were non-applicable to setting #1 since it is a control with transmitted illumination (brightfield).

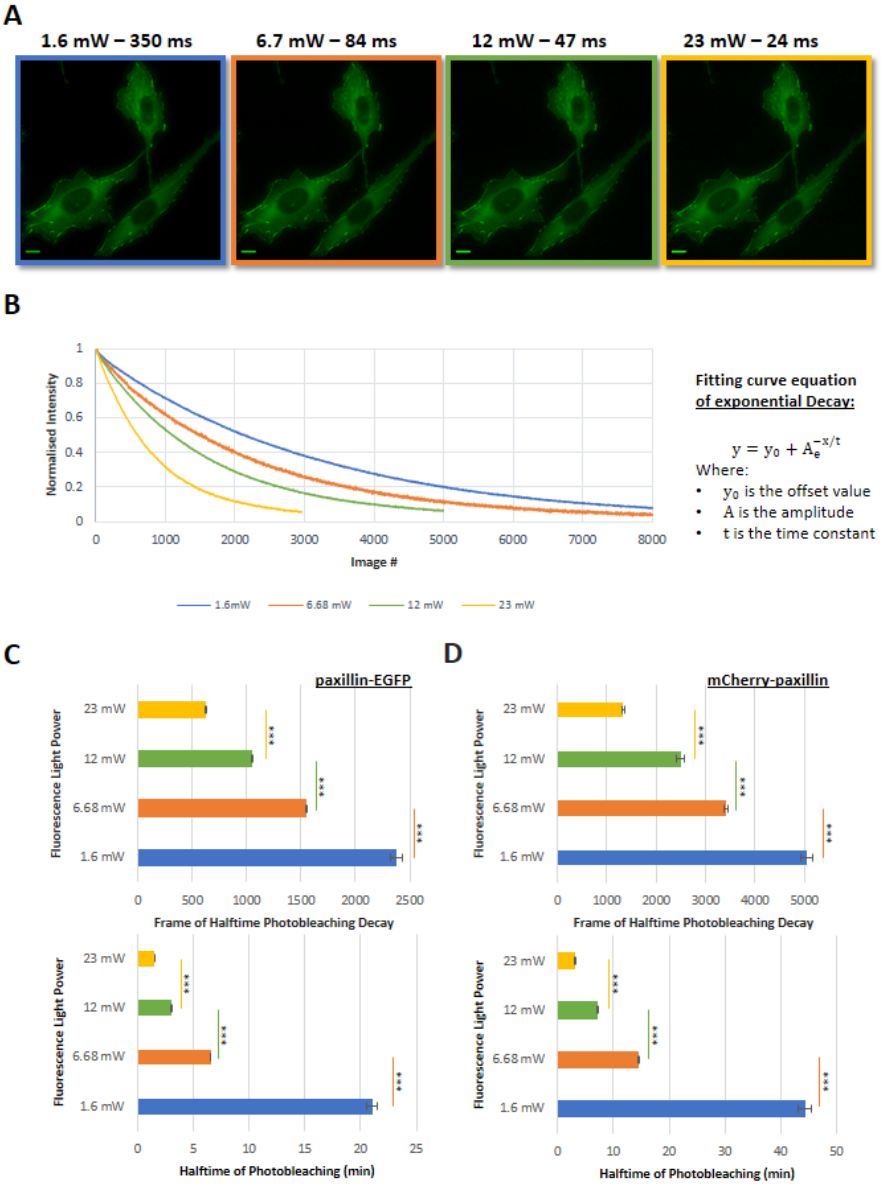

Figure 3.1: Decreasing excitation light power reduces photobleaching of fluorophores. Halftime of the photobleaching decay of fixed CHO-K1 cells with different fluorescent labels measured under illumination conditions described in Table 3.1. (A) Representative images for fixed CHO-K1 cells expressing paxillin-EGFP under imaging settings in Table 3.1. (B) Photobleaching decay curves for fixed CHO-K1 cells expressing paxillin-EGFP. (C) Halftime photobleaching decay in images and time for fixed CHO-K1 cells expressing paxillin-EGFP. (D) Halftime photobleaching decay in images and time for fixed CHO-K1 cells expressing mCherry-paxillin. Experiments are in triplicate with n=21 regions of interest analysed per setting. Error bars are the standard error of the mean. Statistical significance is based on a two-tailed, *t*-test (*P*-values). * represents P<0.05, ** represents P<0.01 and *** represents P<0.001.

This study was expanded to investigate if reduced photobleaching would translate into reduced phototoxicity in living cellular samples when low light powers were used. The brightfield transmitted light imaging technique was used as a complementary control for comparison with the same four settings previously described (Table 3.1). Brightfield illumination is a useful control as it does not induce the fluorescence process nor its undesired phototoxic reactions. Therefore, it was used as a reference in live cellular assays to determine the level of physiological stress endured under various fluorescence imaging conditions. The live cell migration assay was performed by imaging cells at intervals of 2 minutes for a total time of at least 4 hours using a 20x/0.8 NA objective lens. CHO-K1 cells expressing no fluorescent dye or protein imaged in brightfield illumination migrated at a speed of 21 µm/hr (Fig.3.2A). CHO-K1 cells expressing the paxillin-EGFP protein construct imaged using brightfield illumination also migrated with an average speed of 21 µm/hr, which indicated that the presence of the fluorescent protein tagged paxillin-EGFP itself had no notable effect on the process of cell migration. Phototoxicity was detectable when cells were imaged using higher fluorescence light powers of 12 mW and 23 mW at which cells had speeds of 10 µm/hr (Fig. 3.2A). Fluorescence imaging using the intermediate light power of 6.7 mW showed migration speeds that were closer to brightfield control speeds at 15.8 µm/hr (Fig. 3.2A). However, using the lowest light power of 1.6 mW completely restored normal migration speeds of 22 µm/hr (Fig. 3.2A). Rose plots depicting individual cell migration tracks all beginning at the origin point (0,0) showed that cells imaged with brightfield and the low light power setting of 1.6 mW had longer net displacements and moved faster than cells imaged with the higher power 12 mW fluorescence illumination setting (Fig. 3.2B). These findings indicate that low light power fluorescence imaging shows no apparent detrimental effects on cell migration, as opposed to some phototoxicity leading to slower migration speeds with the use of higher light powers.

To complement the results from the migration experiments, another live cell assay was performed. The physiological process of cellular protrusion is known to be sensitive to fluorescence imaging, as cells exposed to excessive illumination form unusually slow and infrequent protrusions[56]. Artifacts of phototoxicity can be seen in protrusion speeds within 30 minutes of imaging, therefore cells were imaged with that time duration at an interval of 20 s using a 20x/0.8 NA objective lens. The imaging conditions used for the cell migration experiments were used here as well (Table 3.1), and protrusion speeds were measured using a kymograph analysis. CHO-K1 cells expressing no fluorescent dye or protein imaged in brightfield illumination formed protrusions at an average speed of 2.0 µm/min and as with the cell migration experiments the presence of the paxillin-EGFP protein construct did not affect migration speeds (Fig. 3.2C). Although cell protrusion was not as sensitive to the light power as cell migration

phototoxicity became evident with the highest light power fluorescence imaging condition of 23 mW. In this case, cells formed protrusions with an average speed of only 1.6 μm/min. Cells imaged with the lower light settings of 12 mw, 6.7 mW and 1.6 mW had similar protrusion speeds to those imaged with brightfield illumination. Intriguingly, cells imaged with the 1.6 mW light setting displayed slightly faster protrusions speeds with an average of 2.3 μm/min. This is likely due to the high variability of protrusion rates from cell-to-cell and event-to-event. The difference in sensitivity between assays highlights the importance of performing multiple tests to determine potential phototoxic effects. The general applicability of light power dependent reduced phototoxicity was verified with CHO-K1-paxillin-mCherry expressing cells. As with EGFP, cells expressing paxillin-mCherry imaged with low light levels protruded with faster speeds than those imaged using higher light powers (Fig. 3.2D). In line with results seen from migration experiments, these results support the hypothesis wherein low light powers coupled to high exposure times are less harmful to cells than high light powers with short exposure times.

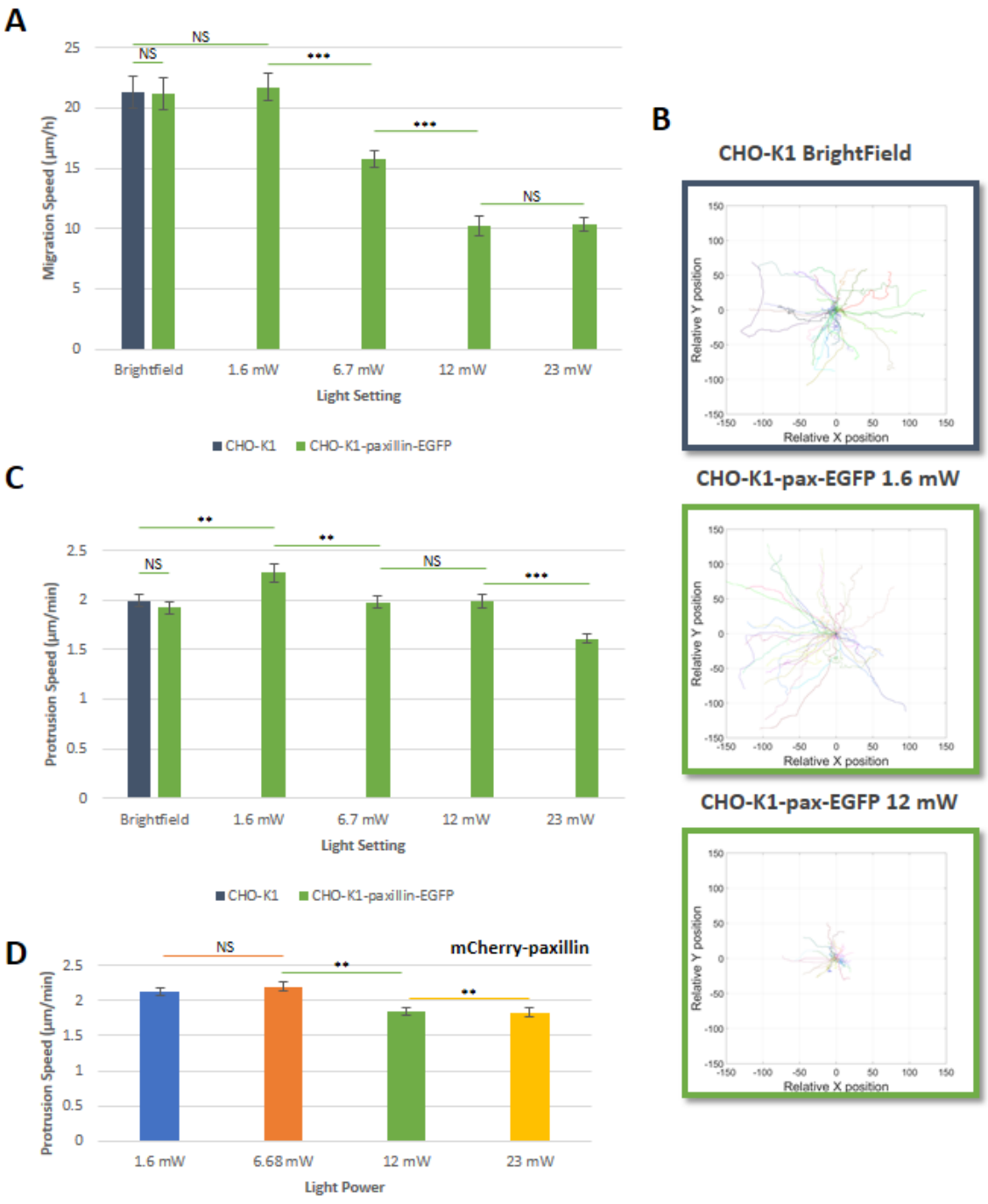

Figure 3.2: Decreasing excitation light powers reduces phototoxicity from fluorophores. Migration and protrusion speed of live CHO-K1 cells with different fluorescent labels measured under illumination conditions described in Table 3.1. (A) Migration speed of live CHO-K1 cells expressing paxillin-EGFP. (B) Rose Plots depicting migration tracks of CHO-K1 paxillin-EGFP cells measured in A. Each line presents the path of a single cell over 2-6 hours. All starting points were superimposed on the origin (0,0). (C) Protrusion speed of live CHO-K1 cells expressing paxillin-EGFP. (D) Protrusion speed of live CHO-K1 cells expressing mCherry-paxillin. Experiments are in triplicate with n >30 cells analysed per setting. Error bars are the standard error of the mean. Statistical significance is based on a two-tailed, *t*-test (*P*-values). * represents P<0.05, ** represents P<0.01 and *** represents P<0.001.

Organic molecules in cells or in tissue culture media other than fluorophores can also absorb light and release toxic by-products that can contribute to overall phototoxicity in a sample. This was observed when imaging CHO-K1 cells expressing no fluorescent dye or protein using the 12 mW higher light setting. Even though no fluorophore was present, toxicity was detected as cells moved at a lower speed of 16 µm/hr (Fig. 3.3A). Similarly, photobleaching of fluorophores can be accelerated by toxic by-products from light absorption and emission of other components in the sample media. This was observed in fixed CHO-K1-paxillin-EGFP expressing cells where serum and phenol red in the media contributed to enhanced EGFP photobleaching (Fig. 3.3B). Serum-free media mounting yielded a 40% increase in the halftime of photobleaching (from 427 to 597 image frames, or from 2 to 2.4 minutes) with full growth media (Fig. 3.3B). This indicates one or several components in the serum can contribute to overall photobleaching and likely also phototoxicity during fluorescence imaging. Similarly, phenol red-free media mounting yielded a 75% increase in the halftime photobleaching from 427 to 750 image frames (or from 2 to minutes) which indicated that phenol red is a specific component that can enhance photobleaching of EGFP (Fig. 3.3B). Moving on, this study investigated whether using the low light technique was also effective at reducing photodamage resulting from sample components other than fluorophores. Photobleaching experiments were performed with cells mounted in regular growth media, serum-free media and phenol-red free media with various incident light powers (Table 3.1). Using lower light powers decreased photobleaching rates in all the mountings used, which indicates that this technique has a general effect of reducing the number of toxic by-products from all sources in a sample (Fig. 3.3C). Furthermore, results indicate that reducing light power is more effective than removing specific components in the sample to reduce their phototoxicity contribution. For instance, removing phenol red from the mounting media decreased photobleaching by 75% compared to full growth media when the 6.7 mW power setting was used, but simply using the lower light setting of 1.6 mW with full growth media decreased photobleaching by 130%, counting image frames (Fig. 3.3C). The better efficiency of using low light power becomes more pronounced when high light powers are used. For example, removing phenol red decreased photobleaching by 24 % (from 176 to 218 image frames) compared to full growth media when the 23 mW light power setting was used, but using the lower light setting of 1.6 mW with full growth media decreased it by 457% (from 176 to 979 image frames, or from 0.6 to 9.3 minutes). The full panel of results comparing all mounting media options used, including PBS is shown in Figure 3.3D. Using PBS as a mounting media yielded the slowest photobleaching rates, which is expected as this buffer does not contain readily available light absorbing molecules that could contribute to phototoxicity (Fig. 3.3C). Although mounting samples in PBS shows the most significant reduction in photobleaching, it is not a

viable option for live cell imaging due to the lack of essential nutrients. Overall, these results show that it is important to evaluate how different components in the cell media contribute to photobleaching and phototoxicity. However, if significantly low light powers are used these secondary toxicity effects from the mounting media components become less relevant.

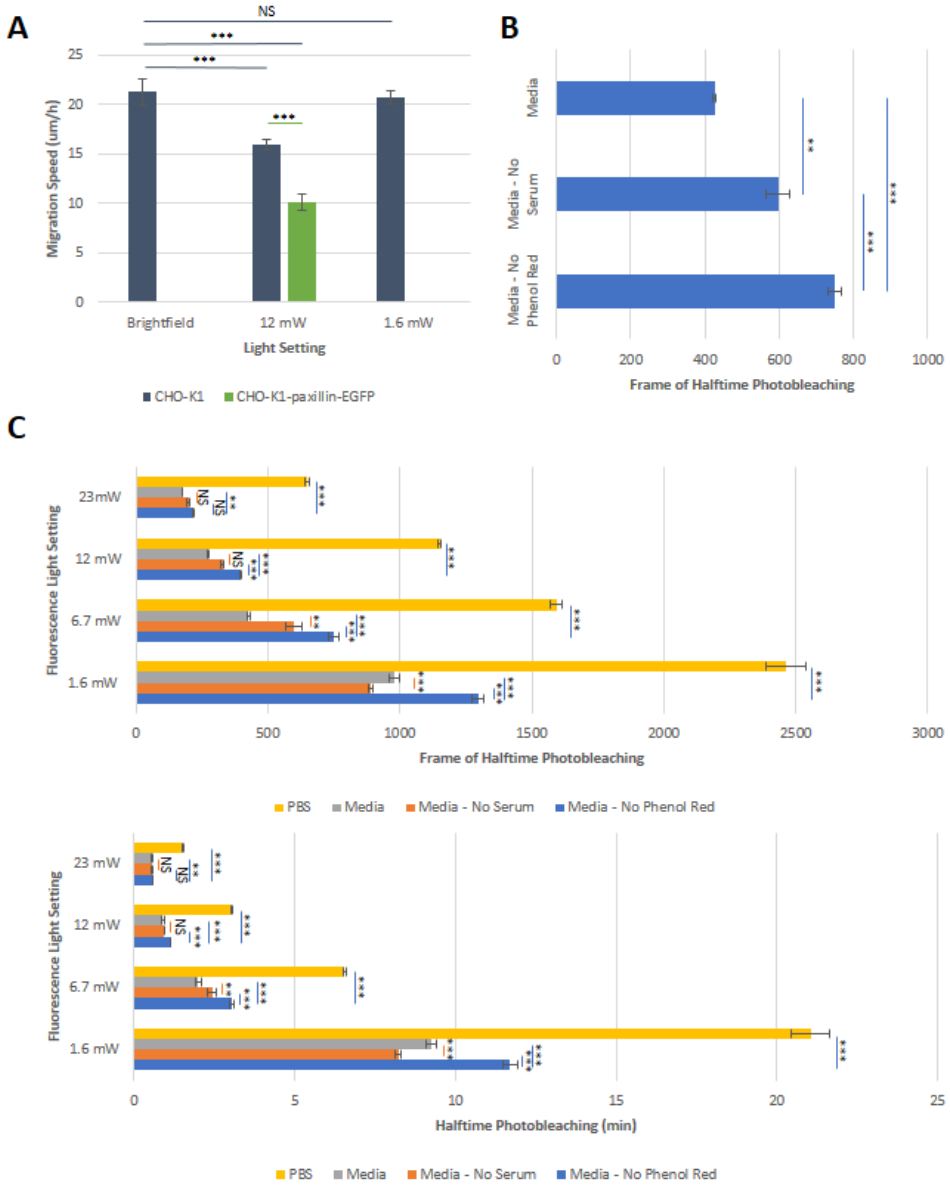

Figure 3.3: Decreasing excitation light powers is more efficient at reducing phototoxicity and photobleaching than removing reactive mounting media components. Migration speed of live CHO-K1 cells and halftime of the photobleaching decay of fixed cells measured under illumination conditions described in Table 3.1 when mounted either in PBS, full growth media, serum free media or phenol red free media. (A) Migration speed of live CHO-K1 cells expressing no fluorescent probe or paxillin-EGFP. (B) Halftime photobleaching decay in images for fixed CHO-K1 cells expressing paxillin-EGFP measured under illumination condition #4 in Table 3.1. (C) Halftime photobleaching decay in images and time for fixed CHO-K1 cells expressing paxillin-EGFP under all illumination conditions in Table 3.1. Experiments are in triplicate with n >30 cells analysed for migration experiments and n=21 regions of interest analysed per setting for photobleaching experiments. Error bars are the standard error of the mean. Statistical significance is based on a two-tailed, *t*-test (*P*-values). * represents P<0.05, ** represents P<0.01 and *** represents P<0.001.

3.2–Comparison to other techniques typically used to reduce photobleaching and phototoxicity

In general, it is better to reduce light levels and not add extraneous chemicals to living biological systems under study. However, experiments were performed to compare the techniques presented here with other commercially available solutions. The technique was compared to the use of the ProLong Live™ reagent that functions by metabolising singlet oxygen radicals in the media to prevent their reaction with cellular components or molecules in the media leading to photobleaching and phototoxicity. Photobleaching experiments were replicated with fixed CHO-K1-paxillin-EGFP expressing cells mounted either in regular media or in media supplemented with the ProLong Live™ reagent using the 4 widefield fluorescence imaging light settings (Table 3.1). Photobleaching rates were modestly decreased across all light settings in the presence of ProLong Live™ although the reduction with 6.7 mW light was not significant (Fig. 3.4A). This data would argue that for these modest reductions in photobleaching it would be better to simply reduce the light power. However, if speed is needed requiring higher light power then the ProLong Live™ reagent would make sense to add. The migration and protrusion assays were replicated to investigate the efficiency of the ProLong Live™ reagent as compared to reducing light power at decreasing phototoxicity. The average migration speed of live CHO-K1-paxillin-EGFP expressing cells slightly increased from 11 μm/hr to 14 μm/hr in the presence of ProLong Live™ with the 12 mW light power setting (Fig. 3.4B). An important implication of this observation is that ProLong Live™ does not lead to complete suppression of phototoxicity, likely because factors other than singlet oxygen radicals contribute towards sample phototoxicity. The presence of ProLong Live™ did not result in any recovery of cell protrusion speeds to comparable levels as the brightfield imaging condition controls (Fig. 3.4C). The inefficiency of ProLong Live™ to recover cell protrusion speeds could be explained by the diverse photophysical processes that fluorophores can undergo. Overall, these results show that using ProLong Live™ to reduce photodamage is not as effective as using an all-encompassing solution such as low light power.

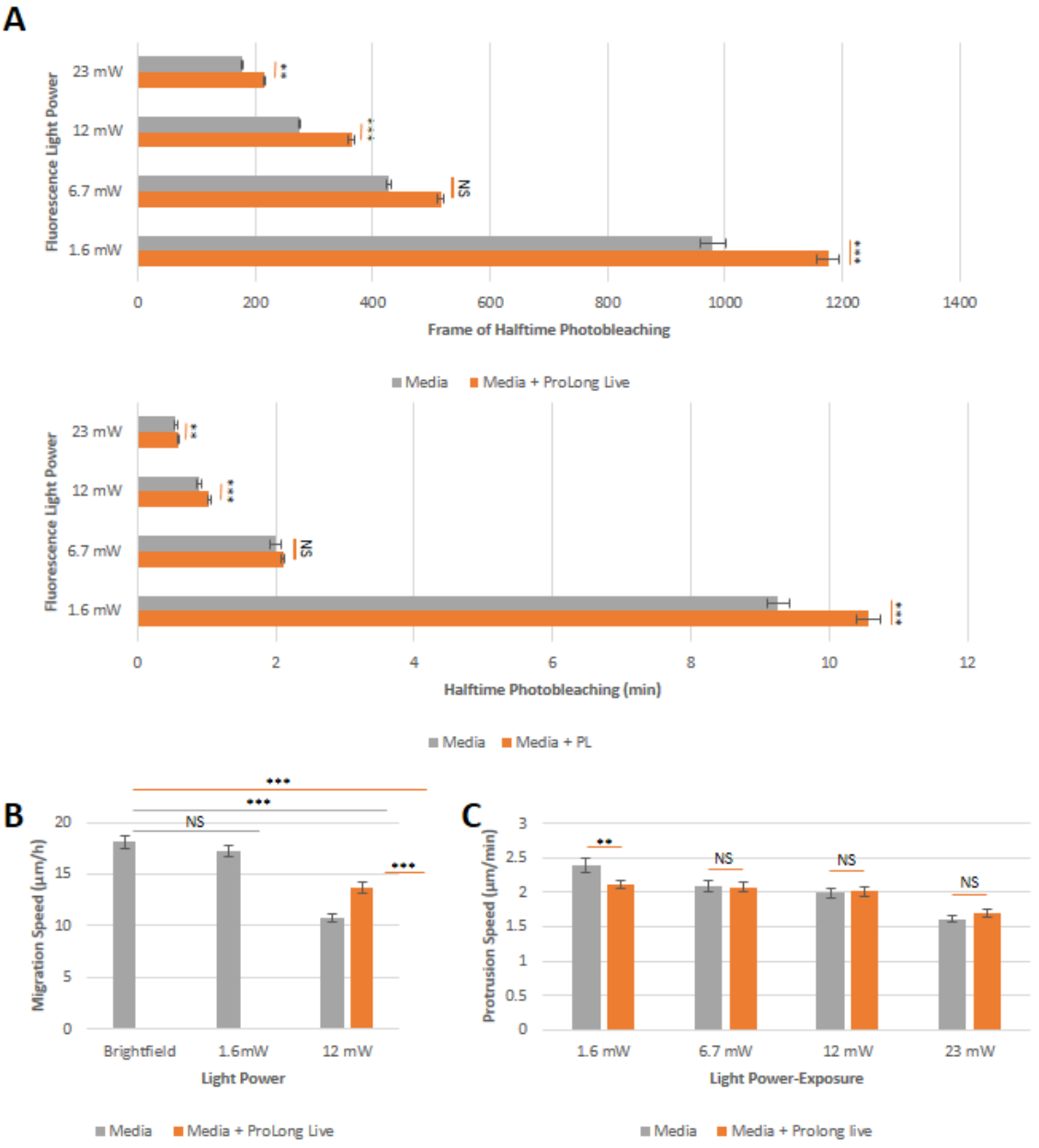

Figure 3.4: Decreasing excitation light power is more efficient at reducing phototoxicity and photobleaching than the single oxygen species scavenger ProLong Live™. Migration and protrusion speed of live CHO-K1 cells and halftime of the photobleaching decay of fixed cells measured under illumination conditions described in Table 3.1 with and without the singlet oxygen scavenger ProLong Live™. (A) Halftime photobleaching decay in images and time for fixed CHO-K1 cells expressing paxillin-EGFP. (B) Migration speed of live CHO-K1 cells expressing paxillin-EGFP. (C) Protrusion speed of live CHO-K1 cells expressing paxillin-EGFP. Experiments are in triplicate with n >25 cells analysed for migration and protrusion experiments and n=21 regions of interest analysed per setting for photobleaching experiments. Error bars are the standard error of the mean. Statistical significance is based on a two-tailed, *t*-test (*P*-values). * represents P<0.05, ** represents P<0.01 and *** represents P<0.001.

3.3 – Low laser powers and longer pixel dwell times decrease photobleaching and phototoxicity of laser scanning confocal microscopy

Results shown in Section 3.1 were collected using widefield fluorescence microscopy. However, photobleaching and phototoxicity can be even more prevalent in confocal microscopy where the focused laser beams have a very high photon density. Each pixel is collected one at a time and fluorophores are excited with a high photon flux in a volume of approximately one femtoliter. This study was expanded to investigate the efficiency of using the principle of lower laser powers and longer exposure times to decrease photobleaching. Three different laser scanning confocal imaging settings were used (Table 3.2). The settings moved from a high laser power of 237 µW to moderate 44 µW and low power 20 µW as measured with a 10x/0.3 NA microscope lens. The pixel times were set to provide a comparable number of photons delivered per pixel (see Section 2.2.3). The pixel dwell times were 4.4 µs 24 µs and 53 µs, respectively. These imaging conditions resulted in nearly identical quality of image and signal-to-noise for the same field of view of fixed CHO-K1-paxillin-EGFP expressing cells (Fig. 3.5A). Photobleaching experiments were performed using samples of these cells imaged with a 60x/1.4 NA oil immersion objective lens under these laser power conditions. Halftime for photobleaching of 27, 63 and 84 image frames were observed for laser powers of 237 µW, 44 µW and 20 µW, respectively (Fig. 3.5B). In line with previous results, using the lowest laser power resulted in the slowest photobleaching rate with a 2-fold improvement from the highest laser power with no compromise in image quality. Further testing was done to investigate if using lower laser power also reduced phototoxicity in live cells. The protrusion assay was performed on CHO-K1 paxillin-EGFP expressing cells imaged every 20 s for 30 minute using a 20x/0.75 NA objective lens. Cells protruded with an average speed of 1.51 µm/min when imaged with the 237 µW laser setting (Fig. 3.5C). Cells protruded with a significantly higher speed of 2.2 µm/min 44 or 20 µW powers were used. This shows the efficiency of this approach at reducing phototoxicity in addition to photobleaching. The photobleaching assay was repeated with 3 additional fluorophores to verify the general applicability of the technique. CHO-K1-mCherry-paxillin expressing cells, CHO-K1 cells stained with MitoTracker Red™, or CHO-K1 cells stained with the LysoTracker Red™ dye showed a similar trend with reduced photobleaching with lower laser powers. The photobleaching was reduced by 94%, 45% and 13% when compared between the lowest and highest laser power for EGFP, MitoTracker Red™, or LysoTracker Red™, respectively (Fig. 3.5D-E). In general, the technique is effective but the inefficiency of this technique with the LysoTracker Red™ dye could be explained by its inherently low photostability. Overall, this is a viable method to reduce photobleaching and phototoxicity to samples however it is not as practical as the

widefield technique because the reductions are not as significant and the image acquisition times can be long.

	Illumination Setting		
	#1	#2	#3
Pixel Dwell (µs)	4.4	24	53
Light Power (µW)	237	44	20

Table 3.2: Illumination conditions with scaled laser light powers. Illumination conditions were designed with different laser light powers, and pixel dwell times (light exposure) were scaled for all settings to deliver a set number of 2.56 x 10^9 photons per image for EGFP, and 2.94 x 10^9 for mCherry, MitoTracker Red™ and LysoTracker Red™ (see Chapter 2.2.3).

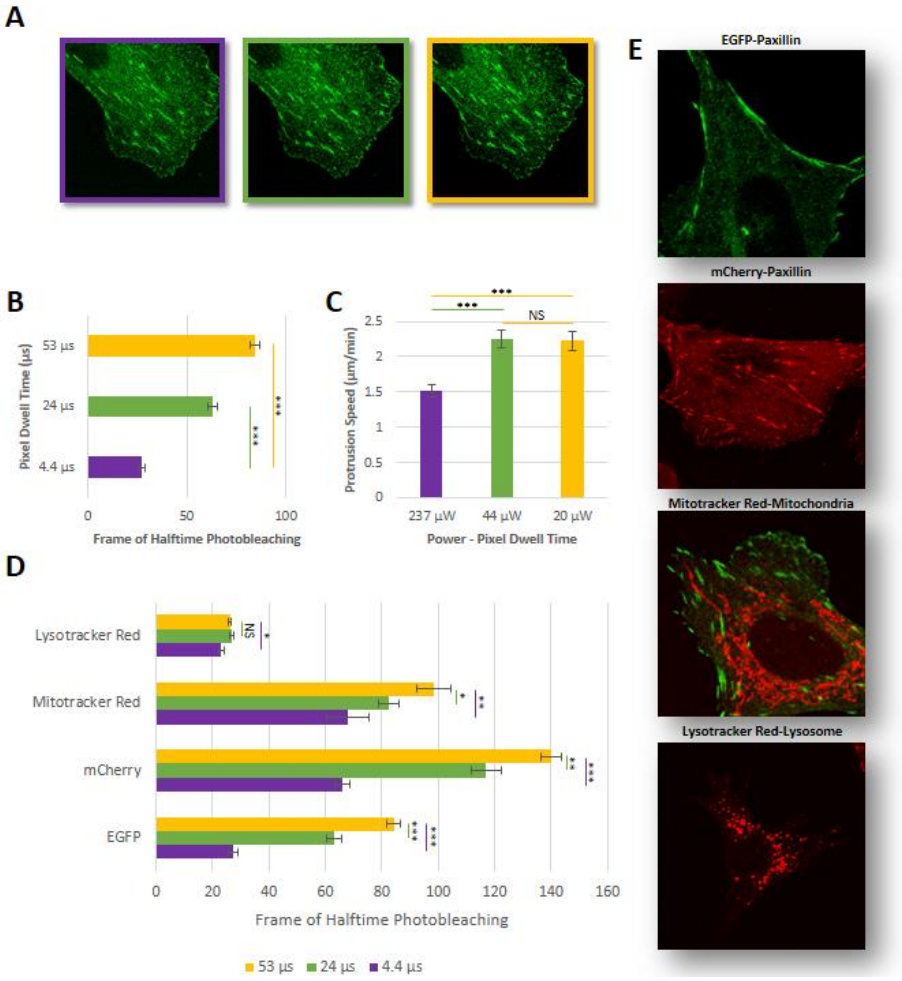

Figure 3.5: Decreasing excitation laser power reduces phototoxicity and photobleaching from fluorophores in confocal microscopy. Halftime of the photobleaching decay of fixed CHO-K1 cells and protrusion speed of live cells with different fluorescent labels measured under illumination conditions described in Table 3.2. (A) Representative images for fixed CHO-K1 cells expressing paxillin-EGFP. (B) Halftime photobleaching decay in images for fixed CHO-K1 cells expressing paxillin-EGFP. (C) Protrusion speed of live CHO-K1 cells expressing paxillin-EGFP. (D) Halftime photobleaching decay in images for fixed CHO-K1 cells expressing paxillin-EGFP, mCherry-paxillin, MitoTracker Red™ and LysoTracker Red™. (E) Representative images of fluorescent probes used in D. Experiments are in triplicate with n >30 cells analysed for protrusion experiments and n=21 regions of interest analysed per setting for photobleaching experiments. Error bars are the standard error of the mean. Statistical significance is based on a two-tailed, *t*-test (*P*-values). * represents P<0.05, ** represents P<0.01 and *** represents P<0.001.

Chapter 4

Results: Pulsed Illumination and Phototoxicity

4.1 – Small pulse widths, and long rest times between pulses decrease photobleaching

The hypothesis that was tested in this section was that millisecond scale pulsing of light during image acquisition can reduce photobleaching and phototoxicity of fluorophores or fluorescent proteins. To investigate this idea, four settings for fluorescence imaging were designed (Table 4.1). The first setting reflected typical illumination with no light pulsing within a designated light exposure time during image acquisition. The remaining three settings exhibited a periodic wave function, known as a square pulse, which was introduced using a pulse generator that was pre-built into the light source. The pulse width was set to 100 µs, 50 µs or 25 µs with an "off/rest time", or dark period of 100 µs between each pulse. Therefore, one pulsing cycle consisted of 25, 50 or 100 µs with the light on, and 100 µs with the light off, and this pulsing was maintained during the image exposure time. A schematic of these illumination settings is shown in Fig. 4.1A. Regardless of the objective lens used for imaging, the incident light power was set to 22 mW as measured with a 10x/0.3 NA objective lens. Due to the fact that the pulse width was varied between settings, the image exposure time was adjusted for each image acquisition setting so that the sample was exposed to the same total amount of light. This allowed for an accurate comparison of photobleaching rates. For example, if the light was pulsed for 100 µs with an off time of 100 µs then the light was on 50% of the time. However, if the light was on for 25 µs with an off time of 100 µs then the light was only on 20% of the time. In this case, the exposure time would have to be 2.5 times longer to maintain the same number of photons hitting the sample during one image acquisition (Methods, Section 2.2.3).

	Illumination Setting			
	#1	#2	#3	#4
Pulse Duration (µs)	No Pulsing	100	50	25
Rest Time Between Pulses (µs)	NA	100	100	100
Exposure Time (ms)	26	56	86	147

Table 4.1: Illumination conditions with pulsing settings with scaled pulse duration. Illumination conditions were designed to maintain the same rest time between pulses but vary the pulse durations. Power was set to 22 mW in all settings, and the total illumination time excluding rest time between pulses was 25.5 ms. Exposure times were scaled for all settings to deliver a set number of 1.33×10^{15} photons per image for cells expressing EGFP, and 1.63×10^{15} for cells expressing mCherry and MitoTracker Red™ (see Chapter 2.2.3).

The photobleaching assay was performed with a 63x/1.4 NA oil immersion objective lens on fixed CHO-K1-paxillin-EGFP expressing cells using the four settings described (Table 4.1). The halftime of photobleaching was 117 image frames (0.7 minutes) with no pulsing or continuous illumination. However, the half time of photobleaching decreased by 81% to 212 image frames (1.3 minutes) with light pulses of 100 µs, 277 frames (1.8 minutes) with 50 µs pulses and 345 frames (2.5 minutes) with 25 µs pulses (Fig. 4.1B). Experiments in this study only went up to 25 µs pulse widths as this was the fastest possible setting with the light source. These results demonstrate that pulsing fluorescence excitation light is a powerful way to reduce EGFP fluorescence photobleaching in widefield microscopy (Fig. 4.1C). In general, the results show that the faster the light pulse width the slower the photobleaching of EGFP. Perhaps the rate could be even further reduced with short pulse widths. The general applicability of light pulsing to reduce photobleaching was tested with CHO-K1 cells stained with MitoTracker Red™ dye or cells expressing mCherry-paxillin (Fig. 4.1D). As with the EGFP, briefer pulse durations resulted in slower photobleaching rates for both fluorescent molecules (Fig. 4.1D).

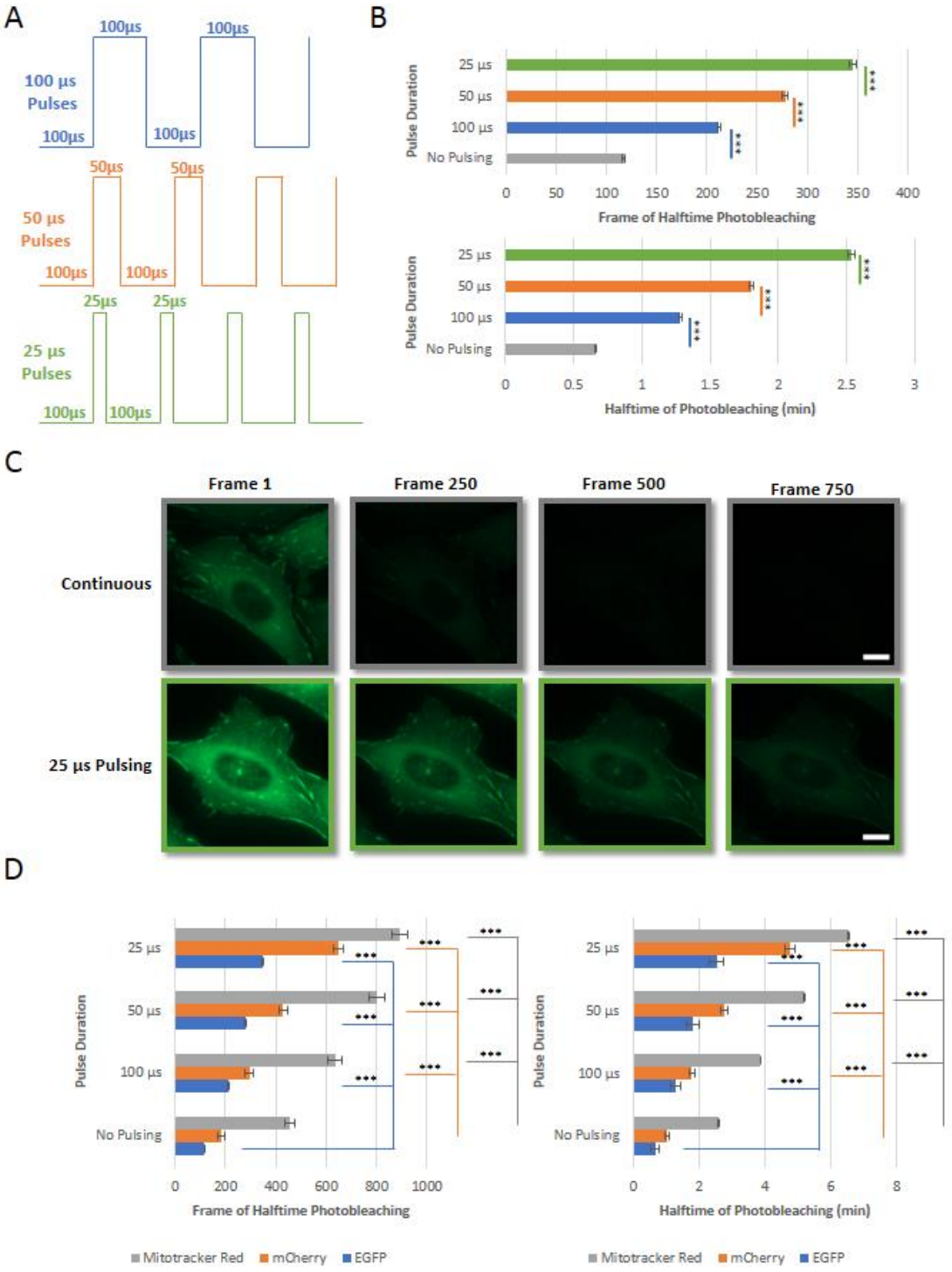

Figure 4.1: Decreasing exciting light pulses reduces photobleaching of fluorophores. Halftime of the photobleaching decay of fixed CHO-K1 cells with different fluorescent labels measured under illumination conditions described in Table 4.1. (A) Schematic representation of the light pulsing cycles used. (B) Halftime photobleaching decay in images and time for fixed CHO-K1 cells expressing paxillin-EGFP. (C) Montage of image frames from selected photobleaching time series with non-pulsed illumination and 25 µs pulses. Images were collected with a 63x/1.4 NA objective lens. (D) Halftime of photobleaching decay in images and time for paxillin-mCherry and MitoTracker Red™ (fluorescent mitochondrial marker). Experiments are in triplicate with n=21 regions of interest analysed per setting. Error bars are the standard error of the mean. Statistical significance is based on a two-tailed, *t*-test (*P*-values). * represents P<0.05, ** represents P<0.01 and *** represents P<0.001.

Modulation of the rest time between pulses was also tested as a possible factor to reduce photobleaching and phototoxicity. Seven different imaging settings were used (Table 4.2): The first was no pulse or continuous illumination, followed by 6 other settings with pulsing cycles of 100 µs on time with off times ranging from 25 µs to 300 µs (Table 4.2, Fig. 4.2A). Because more settings were tested, power was set to 17 mW in this experimental series with a longer exposure time to increase the photon count per image and produce faster photobleaching. In this case, increasing the off time between pulses further reduced the photobleaching rates (Fig. 4.2B). For instance, increasing the rest time between pulses from 100 µs to 300 µs doubled the half time of photobleaching of EGFP (Fig. 4.2B-C). Taken together, these results indicate that rapid pulses followed by long rest periods are ideal for minimizing photobleaching of EGFP.

	Illumination Setting						
	#1	**#2**	**#3**	**#4**	**#5**	**#6**	**#7**
Pulse Duration (µs)	No Pulsing	100	100	100	100	100	100
Rest Time Between Pulses (µs)	/	25	50	100	150	200	300
Exposure Time (ms)	46	66	77	100	123	146	191

Table 4.2: Illumination conditions with pulsing settings with scaled rest time between pulses. Illumination conditions were designed to maintain the same pulse duration but vary the rest times between each pulse. Power was set to 17 mW in all settings, and the total illumination time excluding rest time between pulses was 46 ms. Exposure times were scaled for all settings to deliver a set number of 1.84×10^{15} photons per image (see Chapter 2.2.3).

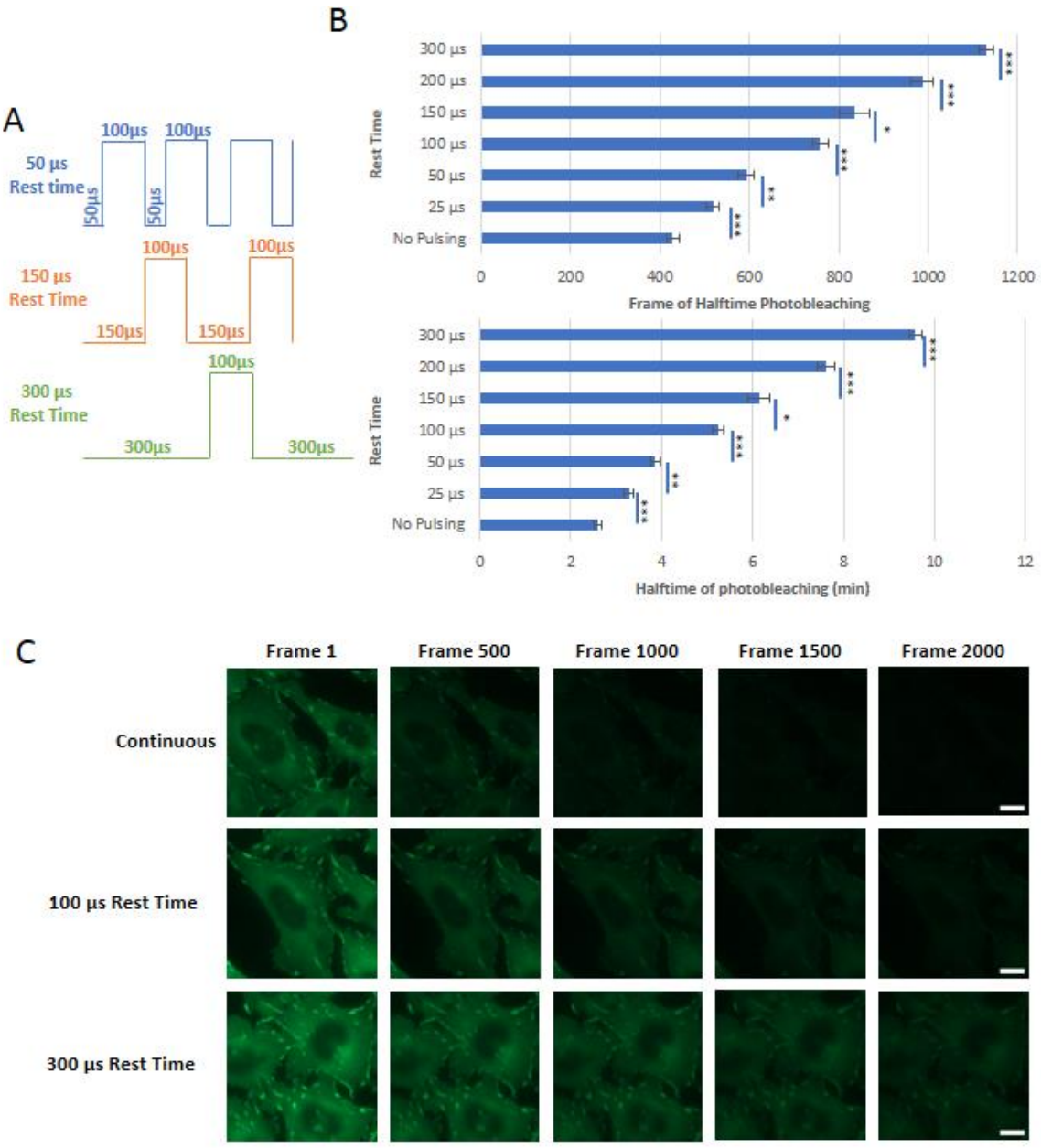

Figure 4.2: Increasing rest time between excitation light pulses reduces photobleaching of EGFP. Halftime of the photobleaching decay of fixed CHO-K1 cells with paxillin-EGFP measured under illumination conditions described in Table 4.2. (A) Schematic representation of the light pulsing cycles used. (B) Halftime photobleaching decay in images and time for fixed CHO-K1 cells expressing paxillin-EGFP. (C) Montage of image frames from selected photobleaching time series with non-pulsed illumination, 150 µs and 300 µs rest time pulsing settings. Experiments are in triplicate with n=21 regions of interest analysed per setting. Error bars are the standard error of the mean. Statistical significance is based on a two-tailed, *t*-test (*P*-values). * represents P<0.05, ** represents P<0.01 and *** represents P<0.001.

4.2 – Small pulse widths, and long rest times between pulses decrease phototoxicity

After investigating reduced photobleaching rates with pulsed illumination, the study was expanded to determine if reduced photobleaching would translate into reduced phototoxicity in live cells. The live cell protrusion assay was conducted with a 20x/0.8 NA objective lens using highly protrusive CHO-K1-paxillin-EGFP expressing cells. The assay was performed with the same pulse width modulation settings described in section 4.1 with a peak power of 22 mW measured with a 10x/0.3 NA objective lens. As shown in Figure 4.3A, kymographs were used to determine the protrusion speed of cells at any point during image acquisition. The protrusion assay demonstrated that cells imaged every 20 seconds with an exposure time of 46 ms without pulsing the light (i.e. continuous illumination) formed protrusions with an average speed of 1.94 μm/hr (Fig. 4.3C). Introducing pulses of 20, 50 or 100 μs with 100 μs rest times between pulses resulted in a 40% increase in the protrusion speed relative to continuous illumination. Unlike in the photobleaching assay, decreasing the pulse width did not show any sign of decreasing phototoxicity or increasing protrusion speeds. It is possible that with the 20 second interval cells are able to recover from any phototoxic effects generated by the fluorescence process or that cell protrusion is not highly sensitive to photobleaching by-products. Other more sensitive live cell phototoxicity assays such as ROS sensors or mitochondrial potential probes could be explored in future studies to measure more subtle cell stress responses.

The effect of changing the rest time between pulses while maintaining the pulse width was also tested with the protrusion assay (Fig. 4.3D). In a similar way, adding a rest time of 150 μs between 100 μs pulses resulted in an increases in protrusion rates (Fig. 4.3E). Pulsed Illumination with a 300 μs rest time between pulses resulted in even faster protrusion speeds. Therefore, increasing rest times between pulses results in less phototoxicity.

Taken together, these results demonstrated that phototoxicity can be reduced by pulsing incident light. Shorter pulses and longer rest times between pulses result in less photobleaching and faster protrusion rates likely due to reduced phototoxicity.

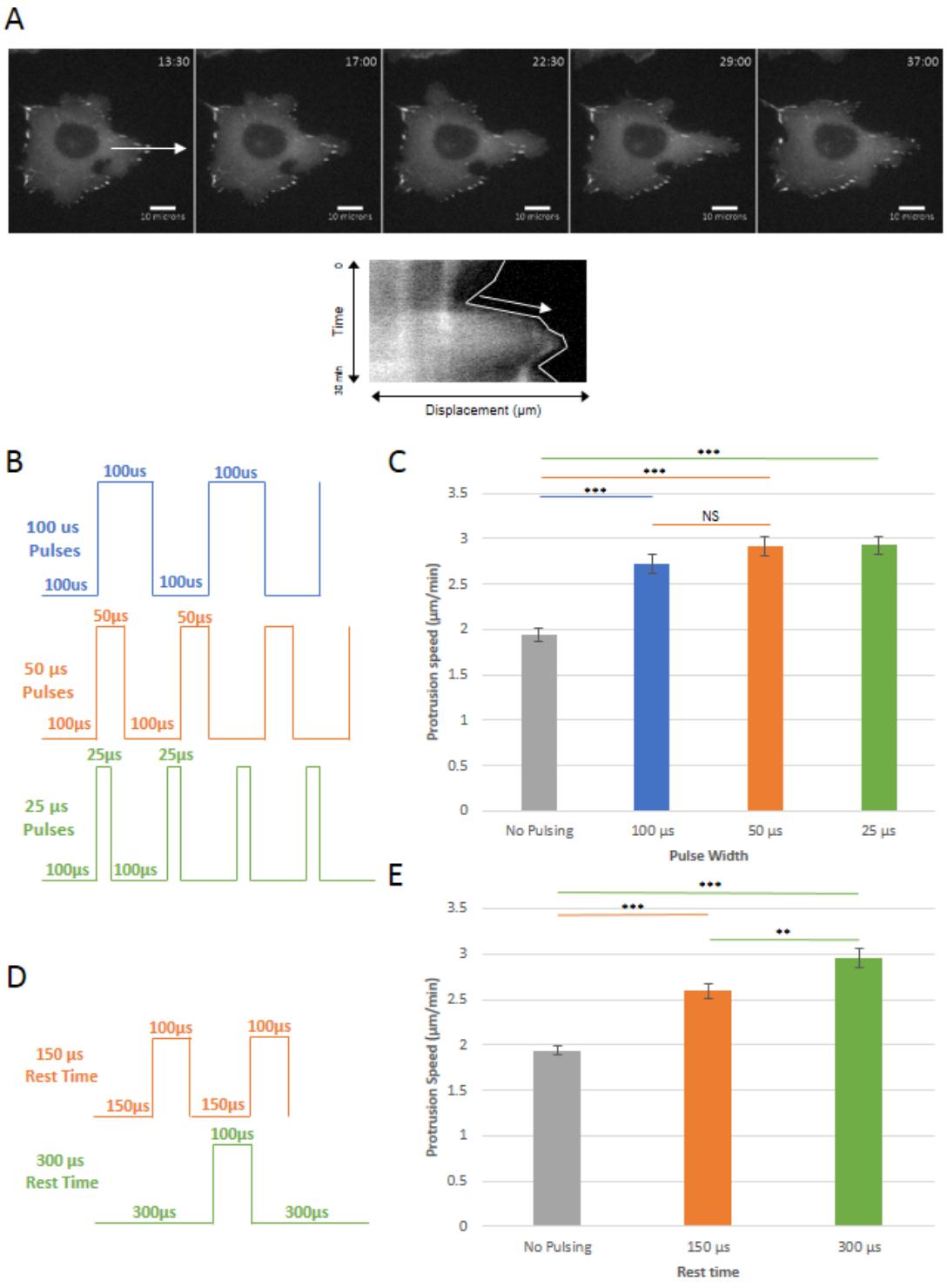

Figure 4.3: Decreasing excitation light pulses and increasing rest time between light pulses reduces phototoxicity from fluorophores. Protrusion speed of live CHO-K1 cells with paxillin-EGFP measured under conditions described in Tables 4.1 and 4.2. (A) Montage of a representative cellular protrusion, with its associated Kymograph showing displacement of the membrane in function of time. (B) Schematic representation of the light pulsing cycles used in C. (C) Protrusion speed of live CHO-K1 cells expressing paxillin-EGFP imaged using light conditions in Table 4.1. (D) Schematic representation of the light pulsing cycles used in E. (E) Protrusion speed of live CHO-K1 cells expressing paxillin-EGFP imaged using light conditions in Table 4.2. Experiments are in triplicate with n >30 cells analysed per setting. Error bars are the standard error of the mean. Statistical significance is based on a two-tailed, *t*-test (*P*-values). * represents P<0.05, ** represents P<0.01 and *** represents P<0.001.

4.3 – Combination of low light power and light pulsing

Lastly, the amplitude of a pulse, or its peak power, was investigated in combination with pulsed light. The light power was set at between 2 mW and 22 mW with pulses of 25 – 100 µs with 100 µs off times. All settings are summarized in Table 4.3. The photobleaching rate of fixed CHO-K1-paxillin-EGFP expressing cells indicated that the effect of reducing light power and pulsing was additive (Fig. 4.4A). For instance, imaging the cells using non-pulsed illumination set at 22 mW power had a halftime photobleaching decay of 311 frames, or 1.8 minutes (Fig. 4.4B). Applying a lower power of 12 mW without pulsing decreased photobleaching further with a halftime of 527 frames (3.2 minutes). When this light power of 12 mW was implemented with the addition of light pulsing at 50 µs width and 100 µs rest time it yielded a much longer halftime photobleaching of 1212 image frames (9.5 minutes). This indicated the effects of these two light modulations were additive with the decrease of power resulting in a 70% improvement but combining that with light pulsing resulting in nearly 3-fold improvement. Additionally, decreasing the power to 6.7 mW whilst maintaining 50 µs pulse width and 100 µs rest times decreased photobleaching with a halftime of 1671 frames (16.3 minutes), and further decreasing of the pulse width to 25 µs extended the halftime of photobleaching decay even more so to 2170 frames (27.8 minutes). Representative montages of the bleaching timeseries for each of these settings are presented in Figure 4.5. In conclusion, using minimal light power and light pulsing is ideal for reduced photobleaching in living samples. A combination of pulsing and low light levels could depend on the time resolution required for experiments. For example, if time is not an issue very low light levels can be applied. However, if a high time resolution is needed a higher power combined with light pulsing may be required to get rapid high signal-to-noise images while minimizing phototoxic effects.

Exposure time per imaging setting (ms)		Pulsing Width Setting (100 µs rest time in all cases)			
		No Pulsing	100 µs	50 µs	25 µs
Light Power Setting	2 mW	280 ms	611 ms	942 ms	1604 ms
	6.7 mW	84 ms	176 ms	268 ms	453 ms
	12 mW	46 ms	100 ms	154 ms	263 ms
	22 mW	26 ms	56 ms	86 ms	146 ms

Table 4.3: Illumination conditions with scaled light powers in addition to pulsing settings with scaled pulse duration. Illumination conditions were designed to maintain the same rest time between pulses but vary the pulse durations. Experiments were replicated at light powers of 2 mW, 6.7 mW, 12 mW and 22 mW. Exposure times were scaled for all settings to deliver a set number of 1.33×10^{15} photons per image (see Chapter 2.2.3).

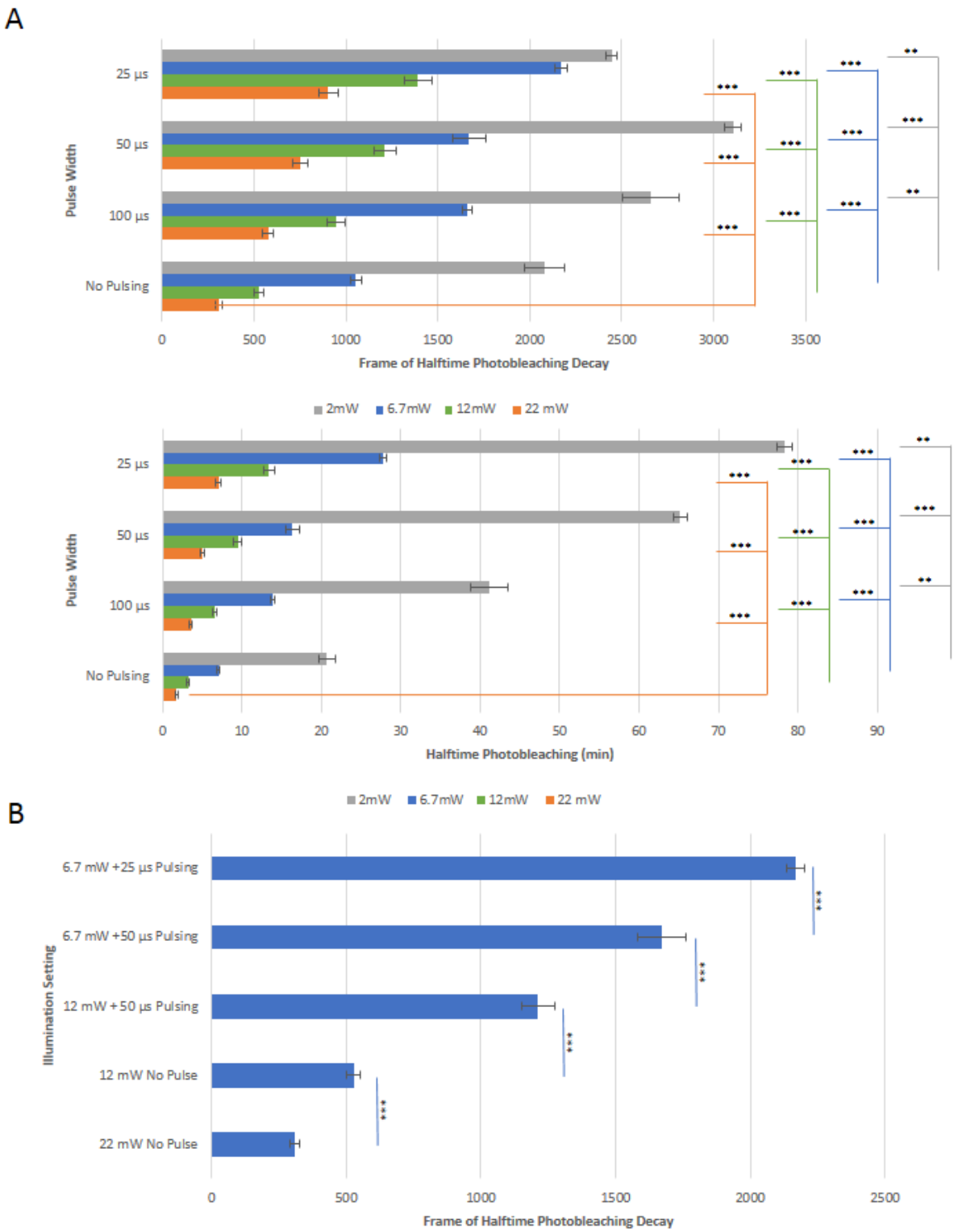

Figure 4.4: Decreasing exciting light pulses and decreasing excitation light power additively reduces photobleaching of EGFP. Halftime of the photobleaching decay of fixed CHO-K1 cells with paxillin-EGFP measured under illumination conditions described in Table 4.3. (A) Halftime photobleaching decay in images and time for fixed CHO-K1 cells expressing paxillin-EGFP. (B) Selected results from A showing the additive effect of the pulsing and low light power techniques. Experiments are in triplicate with n=21 regions of interest analysed per setting. Error bars are the standard error of the mean. Statistical significance is based on a two-tailed, *t*-test (*P*-values). * represents P<0.05, ** represents P<0.01 and *** represents P<0.001.

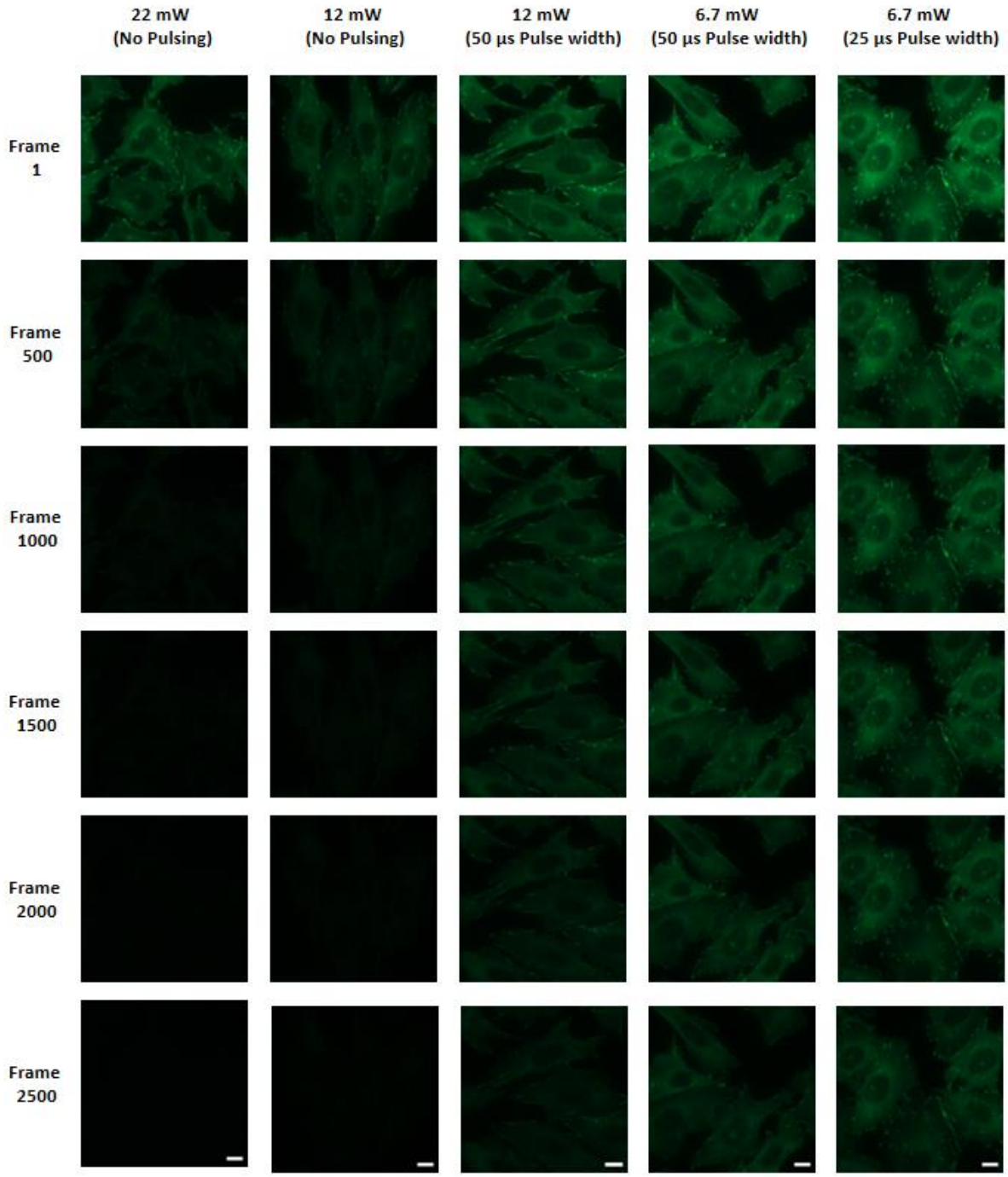

Figure 4.5: Montage of image frames from photobleaching time series in Fig. 4.4B.

Chapter 5

Synthesis and Discussion

5.1 - Low light power technique

Fluorescence microscopy has become an indispensable tool in laboratories, but its use is associated with many challenges due to photobleaching and phototoxicity in imaged samples. Many protocols and techniques attempt to address these shortcomings either through exogenous reagents or instrumental optimisation[46,48,57,58]. However, these solutions can often be incompatible with biological systems or difficult to implement. This study aimed to develop reasonable and non-invasive techniques which could minimize photobleaching and phototoxicity and be broadly applicable across different fluorescence imaging modalities.

The technique developed in Chapter 3 involved the use of low light powers during imaging of CHO-K1-paxillin-EGFP expressing cells to minimize or eliminate damaging photochemical reactions. Results demonstrated that amongst incident light power illumination settings, all of which are comparable in terms of the total number of photons delivered to a sample per image acquisition, those with a low light power and long sample exposure time reduced photobleaching and were less harmful to living systems. The photobleaching reduction was additionally demonstrated for several different fluorescent dyes which shows the general applicability of the technique. In line with a study by Dixit et al. (2003), it was rationalised that imaging samples with low light power would result in a low density of incident photons which would result in a small population of excited fluorophores. Consequentially, the population of more rare dark state molecules would be small, which would result in fewer ROS being produced from downstream reactions. Another factor to consider with live imaging is that cells can up-regulate anti-ROS mechanisms to counter the modestly increased ROS level[40].

Addition of the anti-ROS reagent ProLong Live™ did show some reduction in photobleaching and phototoxicity. This suggests that other ROS-independent photophysical processes are also at play. However, the magnitude of this reduction was not nearly as high as the one seen with the low light technique. The minimal effect of anti-ROS reagents can be explained by the fact that the EGFP chromophore is located on an α-helix protein structure and is completely enclosed within a β-barrel protein structure. This structural feature restricts the mobility of the chromophore and limits accessibility to the solvent and minimizes interactions with neighbouring substrates, including oxygen and ROS[11]. Since photobleaching is still observed in the presence of anti-ROS reagents, the photobleaching of EGFP is likely caused by multiple mechanisms, some that are independent from the production of ROS[59] and the

presence of singlet oxygen. Similar shielding, although probably of different effectiveness depending on the protein structures, is also expected in other fluorescent proteins[60]. The studies here affirmed that using low light power is a generally more effective method to reduce phototoxicity in live samples because it can target ROS-dependent and ROS-independent processes. It also circumvents any potential off-target effects that can ensue from photophysical processes from addition exogenous reagents in the biological system (e.g. media, serum proteins).

5.2 - Light pulsing technique

As elaborated in Chapter 4, another technique that was developed involved excitation of samples using pulsed illumination rather than a continuum of light energy. Previous studies have shown that pulsed laser excitation is effective at reducing photobleaching and phototoxicity[27,61,62]. Results showed that shorter pulses with longer rest times between pulses resulted in reduced photobleaching of fluorescence proteins and organic dyes. Similarly, phototoxicity assays showed that this reduced photobleaching translated to lower phototoxicity, i.e. faster cell migration and membrane protrusion. This is in line with the theoretical framework proposed by Sanden et al. (2007)[63], wherein shorth illumination pulses generate a small population of excited fluorophores which consequently translates into a small population of dark state molecules per pulse cycle. This leads to a low population of excited dark state molecules that can be maintained at low basal levels because they can relax back to the ground state between pulses. Furthermore, allocating more rest time between illumination pulses ensures more of the longer lived dark state species relax back to the ground state and are ready for another round of excitation and fluorescence emission[64]. The magnitude of the impact of the findings of this study on fluorescence imaging became clear when the low light technique and the light pulsing technique were combined. These two techniques together had an additive effect in further reducing photobleaching. This showed that the two methods are likely targeting different photophysical processes. This emphasized the need to further study the individual pathways of photobleaching and phototoxicity to understand the effect of each method.

Although combining both the light power modulation and the light pulsing techniques is highly recommended based on the results presented, this study recognizes the high exposure time limitation that comes with this application. Fortunately, microscopists need only apply 1 of the 2 techniques as the singular effect of either is enough to alleviate phototoxicity and photobleaching in samples. This leaves the question as to which of the two techniques should be prioritized. Naturally, it should always be a

priority to use lower light powers whenever possible as this would minimize the occurrence of the highly damaging multi-photon absorption events. However, this is not always possible. For example, using long exposure times per image acquisition is incompatible with fast, high frequency imaging. Consequentially, using low light power under such conditions would yield very little signal due to the short exposure times. Therefore, in this case the use of pulsed illumination is recommended as it is compatible with the high powers required to produce acceptable images with short exposure times. In all other cases where time resolution is not a limitation, the light power modulation technique is expected to be more beneficial. In fact, it would be pertinent to study the use of constant illumination when imaging by using the lowest light power possible to achieve a good signal to noise ratio with an exposure time matching the time interval between every image acquisition. This would be expected to maximize the effect of the light power modulation technique.

5.3 - Future Directions

5.3.1 - Validation of photophysical properties

Results from chapter 3 and chapter 4 indicate that light intensity plays an important role in promoting or suppressing the various reactions leading to photobleaching and phototoxicity. The next step is to determine which of these reactions are most affected by the light power. The triplet state population of fluorescent probes is the earliest common precursor of all reactions leading to harmful downstream processes including photo-oxidation and ion formation (Fig 1.1) and should therefore be investigated. An important inference from observations made in this study is that the triplet state population of fluorescent probes is considerably larger when light power is increased, given the same number of incident photons per exposure time. This could be verified by directly quantifying the size of this population after exposure to different light powers. The fluorescence correlation spectroscopy (FCS) microscopy technique can be used to investigate this experimentally. FCS uses correlative analysis of spatial and temporal fluctuation in fluorescence intensity to determine molecular properties of a given dye such as its concentration, its diffusion coefficient and the proportion of molecules in the triplet state[65]. The presence of a larger triplet population after application of high light powers would indicate a higher intersystem crossing frequency from the singlet excited state to the triplet state under this illumination condition. Consequently, a larger pool of precursor molecules would lead to a higher number of potentially harmful downstream reactions. Contrarily, a triplet population unaffected by light power would suggest that other photophysical pathways are causing the increased rate of photobleaching and

phototoxicity upon exposure to high light power. Candidates that are potentially involved in this process and that can be further investigated include other molecules or subcellular organelles that are sensitive to light. For example, mitochondria is an organelle that produces ROS for the purpose of cellular signaling and stress response[66]. It is conceivable that this organelle is producing and releasing excessive amount of ROS in response to radiative stress.

Following the characterisation of the triplet population under different light powers, a more detailed study should investigate how specific downstream reaction pathways are affected. For instance, it is well known that ROS-mediated oxidation of fluorophores is one of the main pathways of photobleaching. The effect of light power on this pathway can be studied by measuring the level of ROS accumulation in cells exposed to different light powers. To investigate this experimentally, several quantitative florescent probes for ROS could be used. For example, CellROX™ is a reagent that is non-fluorescent in its ground state but becomes fluorescent once oxidized by ROS. The rate of increase in fluorescence of the CellROX™ reagent and its final fluorescence intensity could then be used to determine the rate of ROS production and ROS quantity within cells, respectively. Of course, imaging of the ROS probe itself could also generate further phototoxicity so carefully designed control experiments would be essential. A linear or exponential increase of ROS as a function of light power would suggest that light power and fluorophore oxidation are directly linked processes. If ROS levels do not increase with light power or attain a plateau after a certain power level, then it would indicate that the oxygen-mediated oxidation mechanism of fluorophores can reach a saturation point after which it is no longer the process responsible for the observed increases in photobleaching and phototoxicity at high light powers. Evidently, all light settings should be designed to deliver the same number of incident photons per image in order to allow for true comparisons between different experiments, as was done in this study.

5.3.2 – Investigating the effect of light power on toxicity

In this study, the common variable used to equilibrate sets of different pulsing settings being compared was that the number of photons delivered per image frame was always equivalent. This was achieved by modulating the exposure time for a given light power whenever the pulse width or rest time was changed to account for the rest time added. The limitation of this method is that power is always constant, which uncouples its effect from the photobleaching and phototoxicity dynamics at play. Increasingly higher light powers are thought to unlock higher order photobleaching and toxic reactions, therefore. In order to further understand this phenomenon and working principle of the pulsing technique, an experimental approach must account for light power. One interesting experimental design

is to compare different illumination settings that are equivalent in the emission intensity per image frame, rather than the number of photons delivered per image frame. That is, the emission intensity and the exposure time between settings would always be constant, but the light power would increase as pulsing is introduced to compensate for the rest time incurred. The equivalent emission intensity would indicate that a similar number of fluorophores underwent the excitation/emission cycles per image frame. As such, any fluctuation in the photobleaching rate would solely be attributed to the power intensity because the exposure time is constant in all cases. If for example the photobleaching rate is similar between a pulsing setting and a continuous light setting, then it can be concluded that the excited fluorophore population size is the main factor to consider in the process of photobleaching. If on the other hand the photobleaching rate is different, it could be suggested that even if a similar number of fluorophores are excited using a higher light power the photon density delivered at such instances adversely affects the fluorescence apparatus (Fig. 1.1). This could be a consequence of an increased intersystem crossing capacity that results in a bigger pool of harmful triplet state molecules. Alternatively, it could be hypothesised that higher order chemical reactions unlocked at higher light powers increase the toxic capacity of a given triplet population. Initial findings (unreported in this study) seem to support the first idea wherein photobleaching rate is identical between continuous and pulsing settings as long as the emission intensity is similar. This should be further studied to shed more light on the underlying photophysical apparatus of the fluorescence process and the workings of the pulsing technique.

5.3.3 - Improvements in phototoxicity assays

Cell migration and protrusion assays were performed to indirectly assess the level of phototoxicity in cells. Results from this study have shown that each of these assays display different levels of toxicity for the same imaging condition. This highlights the importance of considering the sensitivity of tests before making broad conclusions as well as the significance of exploiting multiple assays to verify experimental results. Other assays that can potentially be used to probe phototoxicity levels include testing the viability of cells. For example, the live/dead cell assay involves assessment of a ratio of live to dead cells in an experimental sample in order to determine the health status cells. This viability analysis is easy to implement and allows for a large sampling size. Another method to assess phototoxicity can be the cell cycle analysis[46]. Healthy cells will undergo the cellular division cycle at regular time intervals. However, cells exposed to stress factors can have delayed and decreased division cycles, and some may even fail to divide properly to form multiple nuclei within a single cell. The frequency and regularity of cellular division can be used as a metric to assess the level of phototoxicity. However, it is our opinion that phototoxicity

that leads to effects on cell division would also be easy to measure with the highly sensitive migration and protrusion assays. Another potential test for surveying mild phototoxicity is the 3-(4,5-dimethylthiazol-2-yl)-2,5-diphenyl-tetrazolium bromide (MTT) assay[67]. The MTT salt is readily taken up by cells and reduced by mitochondrial dehydrogenase enzymes to yield a purple colored formazan product that is impermeable to the cellular membrane. Phototoxicity can disturb the cellular membrane and permeabilize it which would then allow the colored formazan to escape. Colorimetric analysis can therefore be used to measure the rate of liberation of the salt to determine the level of toxicity present inside the cell.

5.3.4 – Mathematical modeling of light pulsing

LED light pulsing has been shown to be effective at reducing photobleaching and phototoxicity in fluorescence microscopy. However, a major limitation of this technique is that it requires longer exposure times for optimal implementation. The pulse width would be expected to be most beneficial when kept short, ideally the same duration as the lifetime of the singlet state where no triplet state can absorb a second photon during the same pulse cycle[68]. On the other hand, the rest time would be most effective when it is as long as the longest-lived dark state in order to allow all harmful radicals to relax before the next pulse cycle[68]. In the case of EGFP, this would correspond to a pulse width that is dozens of nanoseconds in duration followed by a rest time as long as 5 milliseconds[68,69]. Therefore, the optimal parameter for pulsing light for this fluorophore would require very long exposure times for a single image, which is evidently not a suitable solution for imaging of many biological processes. However, the pulsing technique can still be effective when parameters are adjusted for individual experimental needs. Future studies should assay the importance of optimizing the pulse width and the rest time relative to each other for specific fluorophores. Mathematical modeling could then follow to show the best compromise for a pulsing setting with an acceptable exposure time to measure the dynamics of the biological process under study.

5.3.5 - Validation of techniques in non-organic fluorescent probes

Apart from organic fluorescent probes, a new generation of synthetic probes are also available for use by microscopists. Nanoparticles, of which quantum dots (QD) are the most popular option, are semiconductor nanocrystals that can fluoresce. The synthetic nature of QD enables flexibility in customizing their design and colour which has yielded high photostability, quantum efficiency and brightness[70]. Quantum dots can be excited with either UV or near UV light and compared to organic dyes, they have narrow emission peaks, which minimizes emission cross-talk and is ideal for multi-color

imaging[14]. Their high photostability, which originates from the different photophysical properties of the fluorescence cycle that these molecules undergo, makes them ideal in high light applications. An interesting development of this study would be to investigate whether the techniques developed here can be applied to nanoparticles as well. If the low light technique has no impact on the bleaching properties of these probes, then it is possible that the strong photostability profile of nanoparticles protects these probes from phototoxicity and also suggests that the pathways targeted in the organic molecular cycle are different than those in these synthetic ones. Such a study would be particularly relevant in further characterizing nanoparticles and contrasting them to their organic counterparts.

5.3.6 - Exploring alternative pulsing patterns

Different patterns of pulsing could be implemented in the light path to elicit a separate effect and efficiency in reducing photobleaching and phototoxicity. In this study, a square pulsating pattern was selected for initial assessment of its various components such as width, rest time and amplitude. Another light pattern that can be implemented is through a sinusoidal pattern during which light intensity would be constantly oscillating. The experiments described in Chapter 3 have demonstrated that using low light powers is very beneficial and it would be expected that a sinusoidal pattern would effectively make use of this as it delivers a big proportion of its light dose under low light power while the power is increasing or decreasing, as opposed to a square pattern's pulse which remains at peak power for the duration of the pulse length. The temporal range of ramp up and down of power could be modified to determine the ideal conditions to minimize photobleaching and phototoxicity. To compare these two patterns, more complex mathematical calculations of the light dose and number of photons per image would be required. Other patterns could also be explored including bell curves or even hybrids of different functions.

5.3.7 - Validation of the efficiency of these techniques in current applications

This study has demonstrated the efficiency of two techniques in reducing damage caused by exposure to fluorescence light through assays which measured the photobleaching rate of fluorophores or the migration speed of cells. An important next step is to investigate the applicability of these techniques on a wider selection of experiments. Adhesion dynamics is a subcellular process wherein adhesions undergo regulated assembly and disassembly to drive cellular motility. Acquiring images of focal adhesion dynamics using long interval time series, which reduces photobleaching and phototoxicity, has limitations as the entire temporal range of adhesion dynamics cannot be captured. This results in sub-optimal quantification of assembly and disassembly rates and cannot account for events faster than the set interval. Further development of the low light power and light pulsing technique with smaller imaging

intervals could be useful for imaging such rapid biological processes as it would increase the temporal resolution of the acquisitions while minimizing the levels of phototoxicity and bleaching. Another biological process that is temporally limited by the length of acquisition is cellular division. Phototoxicity can drastically alter the very complex biological interactions occurring during division and can even bring it to a halt. Furthermore, it is challenging to simultaneously image multiple dyes and accurately track molecular interactions since for every dye, an additional image is required per acquisition, which would add to possible phototoxic effects. The techniques presented in this study are optimized to decrease the amount of phototoxicity generated during each image acquisition, which would then allow for more images to be acquired within a time series and for a higher number of dyes to be simultaneously imaged.

As discussed, this study acknowledges that a major limitation of these techniques is their requirement for long exposure times. Without further optimization, the techniques cannot be fully harnessed in applications that require a very fast time resolution. Calcium imaging applications are such an example where there is a need to capture images at a very high frequency to visualize the very transient calcium propagation events. The pulsing technique could still be applied at fast frequency in this case as the implementation of any type of pulsing in the light path should reduce photobleaching and phototoxicity. Therefore, the pulsing technique could still be used on the condition that pulsing frequencies are determined based on the longest possible exposure time for the biological processes being investigated.

Bibliography

1 Sanderson, M. J., Smith, I., Parker, I. & Bootman, M. D. Fluorescence microscopy. *Cold Spring Harb Protoc* **2014**, pdb top071795, doi:10.1101/pdb.top071795 (2014).

2 McNamara, G., Difilippantonio, M. J. & Ried, T. Microscopy and image analysis. *Curr Protoc Hum Genet* **Chapter 4**, Unit 4 4, doi:10.1002/0471142905.hg0404s46 (2005).

3 Renz, M. Fluorescence microscopy-a historical and technical perspective. *Cytometry A* **83**, 767-779, doi:10.1002/cyto.a.22295 (2013).

4 Combs, C. A. Fluorescence microscopy: a concise guide to current imaging methods. *Curr Protoc Neurosci* **Chapter 2**, Unit2 1, doi:10.1002/0471142301.ns0201s50 (2010).

5 Webb, D. J. & Brown, C. M. Epi-fluorescence microscopy. *Methods Mol Biol* **931**, 29-59, doi:10.1007/978-1-62703-056-4_2 (2013).

6 Diaspro, A., Chirico, G., Usai, C., Ramoino, P. & Dobrucki, J. in *Handbook Of Biological Confocal Microscopy* (ed J. Pawley) 690-702 (Springer, 2006).

7 Stennett, E. M., Ciuba, M. A. & Levitus, M. Photophysical processes in single molecule organic fluorescent probes. *Chem Soc Rev* **43**, 1057-1075, doi:10.1039/c3cs60211g (2014).

8 Eggeling, C., Volkmer, A. & Seidel, C. A. Molecular photobleaching kinetics of Rhodamine 6G by one- and two-photon induced confocal fluorescence microscopy. *Chemphyschem* **6**, 791-804, doi:10.1002/cphc.200400509 (2005).

9 Meech, S. R. Excited state reactions in fluorescent proteins. *Chem Soc Rev* **38**, 2922-2934, doi:10.1039/b820168b (2009).

10 Ha, T. & Tinnefeld, P. Photophysics of fluorescent probes for single-molecule biophysics and super-resolution imaging. *Annu Rev Phys Chem* **63**, 595-617, doi:10.1146/annurev-physchem-032210-103340 (2012).

11 Mamontova, A. V., Grigoryev, A. P., Tsarkova, A. S., Lukyanov, K. A. & Bogdanov, A. M. Struggle for Photostability: Bleaching Mechanisms of Fluorescent Proteins. *Russian Journal of Bioorganic Chemestry* **43**, 625-633 (2017).

12 Lichtman, J. W. & Conchello, J. A. Fluorescence microscopy. *Nat Methods* **2**, 910-919, doi:10.1038/nmeth817 (2005).

13 Berezin, M. Y. & Achilefu, S. Fluorescence lifetime measurements and biological imaging. *Chem Rev* **110**, 2641-2684, doi:10.1021/cr900343z (2010).

14 Toseland, C. P. Fluorescent labeling and modification of proteins. *J Chem Biol* **6**, 85-95, doi:10.1007/s12154-013-0094-5 (2013).

15 Shimomura, O., Johnson, F. H. & Saiga, Y. Extraction, purification and properties of aequorin, a bioluminescent protein from the luminous hydromedusan, Aequorea. *J Cell Comp Physiol* **59**, 223-239 (1962).

16 Kremers, G. J., Gilbert, S. G., Cranfill, P. J., Davidson, M. W. & Piston, D. W. Fluorescent proteins at a glance. *J Cell Sci* **124**, 157-160, doi:10.1242/jcs.072744 (2011).

17 Betzig, E. *et al.* Imaging intracellular fluorescent proteins at nanometer resolution. *Science* **313**, 1642-1645, doi:10.1126/science.1127344 (2006).

18 Song, L., Hennink, E. J., Young, I. T. & Tanke, H. J. Photobleaching kinetics of fluorescein in quantitative fluorescence microscopy. *Biophys J* **68**, 2588-2600, doi:10.1016/S0006-3495(95)80442-X (1995).

19 Eggeling, C., Widengren, J., Rigler, R. & Seidel, C. A. *Applied Fluorescence in Chemestry, Biology and Medicine*. 208-240 (Springer, 1999).

20 Bernas, T., Zarebski, M., Dobrucki, J. W. & Cook, P. R. Minimizing photobleaching during confocal microscopy of fluorescent probes bound to chromatin: role of anoxia and photon flux. *J Microsc* **215**, 281-296, doi:10.1111/j.0022-2720.2004.01377.x (2004).

21 Widengren, J., Chmyrov, A., Eggeling, C., Lofdahl, P. A. & Seidel, C. A. Strategies to improve photostabilities in ultrasensitive fluorescence spectroscopy. *J Phys Chem A* **111**, 429-440, doi:10.1021/jp0646325 (2007).
22 Vogelsang, J. *et al.* A reducing and oxidizing system minimizes photobleaching and blinking of fluorescent dyes. *Angew Chem Int Ed Engl* **47**, 5465-5469, doi:10.1002/anie.200801518 (2008).
23 Eggeling, C. *et al.* Analysis of photobleaching in single-molecule multicolor excitation and Forster resonance energy transfer measurements. *J Phys Chem A* **110**, 2979-2995, doi:10.1021/jp054581w (2006).
24 Kalies, S., Kuetemeyer, K. & Heisterkamp, A. Mechanisms of high-order photobleaching and its relationship to intracellular ablation. *Biomed Opt Express* **2**, 805-816, doi:10.1364/BOE.2.000816 (2011).
25 Deschennes, L. A. & Vanden Bout, D. A. Single molecule photobleaching: increasing photon yield and survival time through suppression of two-step photolysis. *Chemical Physics Letters* **365**, 387-395 (2002).
26 Dittrich, P. S. & Schwille, P. Photobleaching and stabilization of. fluorophores used for single-molecule analysis. with one- and two-photon excitation. *Applied Physics B* **73**, 829-837 (2001).
27 Oracz, J., Westphal, V., Radzewicz, C., Sahl, S. J. & Hell, S. W. Photobleaching in STED nanoscopy and its dependence on the photon flux applied for reversible silencing of the fluorophore. *Sci Rep* **7**, 11354, doi:10.1038/s41598-017-09902-x (2017).
28 Yoshiharu, U., Keiko, I. & Masao, K. Switch-over of the Mechanism of the Primary Processes in the Photo-oxidation of Xanthene Dyes as Revealed by the Oxygen Consumption Experiments *Bulletin of the Chemical Society of Japan* **38**, 974-979 (1965).
29 Zondervan, R., Kulzer, F., Kol'chenk, M. A. & Orrit, M. Photobleaching of Rhodamine 6G in Poly(vinyl alcohol) at the Ensemble and Single-Molecule Levels. *The Journal of Physical Chemistry A* **108**, 1657-1665 (2004).
30 Chudakov, D. M., Matz, M. V., Lukyanov, S. & Lukyanov, K. A. Fluorescent proteins and their applications in imaging living cells and tissues. *Physiol Rev* **90**, 1103-1163, doi:10.1152/physrev.00038.2009 (2010).
31 Gorgidze, L. A., Oshemkova, S. A. & Vorobjev, I. A. Blue light inhibits mitosis in tissue culture cells. *Biosci Rep* **18**, 215-224 (1998).
32 Rosner, J. *et al.* Minimizing photodecomposition of flavin adenine dinucleotide fluorescence by the use of pulsed LEDs. *J Microsc* **264**, 215-223, doi:10.1111/jmi.12436 (2016).
33 Stockley, J. H. *et al.* Surpassing light-induced cell damage in vitro with novel cell culture media. *Sci Rep* **7**, 849, doi:10.1038/s41598-017-00829-x (2017).
34 Grzelak, A., Rychlik, B. & Bartosz, G. Light-dependent generation of reactive oxygen species in cell culture media. *Free Radic Biol Med* **30**, 1418-1425 (2001).
35 Pattison, D. I. & Davies, M. J. Actions of ultraviolet light on cellular structures. *EXS*, 131-157 (2006).
36 Halliwell, B. Reactive species and antioxidants. Redox biology is a fundamental theme of aerobic life. *Plant Physiol* **141**, 312-322, doi:10.1104/pp.106.077073 (2006).
37 Hockberger, P. E. *et al.* Activation of flavin-containing oxidases underlies light-induced production of H2O2 in mammalian cells. *Proc Natl Acad Sci U S A* **96**, 6255-6260 (1999).
38 Godley, B. F. *et al.* Blue light induces mitochondrial DNA damage and free radical production in epithelial cells. *J Biol Chem* **280**, 21061-21066, doi:10.1074/jbc.M502194200 (2005).
39 YBlay, J. & Price, R. B. Cellular inhibition produced by dental curing lights is a heating artifact. *Journal of Biomedical Materials Research Part B: Applied Biomaterials* **93**, 367-374 (2010).

40 Dixit, R. & Cyr, R. Cell damage and reactive oxygen species production induced by fluorescence microscopy: effect on mitosis and guidelines for non-invasive fluorescence microscopy. *Plant J* **36**, 280-290 (2003).
41 Song, L., Varma, C. A., Verhoeven, J. W. & Tanke, H. J. Influence of the triplet excited state on the photobleaching kinetics of fluorescein in microscopy. *Biophys J* **70**, 2959-2968, doi:10.1016/S0006-3495(96)79866-1 (1996).
42 Cordes, T., Vogelsang, J. & Tinnefeld, P. On the mechanism of Trolox as antiblinking and antibleaching reagent. *J Am Chem Soc* **131**, 5018-5019, doi:10.1021/ja809117z (2009).
43 Shi, X., Lim, J. & Ha, T. Acidification of the oxygen scavenging system in single-molecule fluorescence studies: in situ sensing with a ratiometric dual-emission probe. *Anal Chem* **82**, 6132-6138, doi:10.1021/ac1008749 (2010).
44 Aitken, C. E., Marshall, R. A. & Puglisi, J. D. An oxygen scavenging system for improvement of dye stability in single-molecule fluorescence experiments. *Biophys J* **94**, 1826-1835, doi:10.1529/biophysj.107.117689 (2008).
45 Mot, A. I., Liddell, J. R., White, A. R. & Crouch, P. J. Circumventing the Crabtree Effect: A method to induce lactate consumption and increase oxidative phosphorylation in cell culture. *Int J Biochem Cell Biol* **79**, 128-138, doi:10.1016/j.biocel.2016.08.029 (2016).
46 Icha, J., Weber, M., Waters, J. C. & Norden, C. Phototoxicity in live fluorescence microscopy, and how to avoid it. *Bioessays* **39**, doi:10.1002/bies.201700003 (2017).
47 Shaner, N. C., Steinbach, P. A. & Tsien, R. Y. A guide to choosing fluorescent proteins. *Nat Methods* **2**, 905-909, doi:10.1038/nmeth819 (2005).
48 Khodjakov, A. & Rieder, C. L. Imaging the division process in living tissue culture cells. *Methods* **38**, 2-16, doi:10.1016/j.ymeth.2005.07.007 (2006).
49 Waldchen, S., Lehmann, J., Klein, T., van de Linde, S. & Sauer, M. Light-induced cell damage in live-cell super-resolution microscopy. *Sci Rep* **5**, 15348, doi:10.1038/srep15348 (2015).
50 Douthwright, S. & Sluder, G. Live Cell Imaging: Assessing the Phototoxicity of 488 and 546 nm Light and Methods to Alleviate it. *J Cell Physiol* **232**, 2461-2468, doi:10.1002/jcp.25588 (2017).
51 Laissue, P. P., Alghamdi, R. A., Tomancak, P., Reynaud, E. G. & Shroff, H. Assessing phototoxicity in live fluorescence imaging. *Nat Methods* **14**, 657-661, doi:10.1038/nmeth.4344 (2017).
52 Evanko, D. Is phototoxicity compromising exprimental results? *Nature Methods* **23-Nov** (2013).
53 Zheng, Q., Jockusch, S., Zhou, Z. & Blanchard, S. C. The contribution of reactive oxygen species to the photobleaching of organic fluorophores. *Photochem Photobiol* **90**, 448-454, doi:10.1111/php.12204 (2014).
54 Alejo, J. L., Blanchard, S. C. & Andersen, O. S. Small-molecule photostabilizing agents are modifiers of lipid bilayer properties. *Biophys J* **104**, 2410-2418, doi:10.1016/j.bpj.2013.04.039 (2013).
55 Eggeling, C., Widengren, J., Rigler, R. & Seidel, C. A. Photobleaching of Fluorescent Dyes under Conditions Used for Single-Molecule Detection: Evidence of Two-Step Photolysis. *Anal Chem* **70**, 2651-2659, doi:10.1021/ac980027p (1998).
56 Boudreau, C. *et al.* Excitation Light Dose Engineering to Reduce Photo-bleaching and Photo-toxicity. *Sci Rep* **6**, 30892, doi:10.1038/srep30892 (2016).
57 Magidson, V. & Khodjakov, A. Circumventing photodamage in live-cell microscopy. *Methods in cell biology* **114**, 545-560, doi:10.1016/B978-0-12-407761-4.00023-3 (2013).
58 Frigault, M. M., Lacoste, J., Swift, J. L. & Brown, C. M. Live-cell microscopy - tips and tools. *J Cell Sci* **122**, 753-767, doi:122/6/753 [pii] 10.1242/jcs.033837 (2009).
59 Jimenez-Banzo, A., Nonell, S., Hofkens, J. & Flors, C. Singlet oxygen photosensitization by EGFP and its chromophore HBDI. *Biophys J* **94**, 168-172, doi:10.1529/biophysj.107.107128 (2008).

60 Chapagain, P. P., Regmi, C. K. & Castillo, W. Fluorescent protein barrel fluctuations and oxygen diffusion pathways in mCherry. *J Chem Phys* **135**, 235101, doi:10.1063/1.3660197 (2011).
61 Donnert, G., Eggeling, C. & Hell, S. W. Triplet-relaxation microscopy with bunched pulsed excitation. *Photochem Photobiol Sci* **8**, 481-485, doi:10.1039/b903357m (2009).
62 Donnert, G. *et al.* Macromolecular-scale resolution in biological fluorescence microscopy. *Proc Natl Acad Sci U S A* **103**, 11440-11445, doi:10.1073/pnas.0604965103 (2006).
63 Sanden, T., Persson, G., Thyberg, P., Blom, H. & Widengren, J. Monitoring kinetics of highly environment sensitive states of fluorescent molecules by modulated excitation and time-averaged fluorescence intensity recording. *Anal Chem* **79**, 3330-3341, doi:10.1021/ac0622680 (2007).
64 Donnert, G., Eggeling, C. & Hell, S. W. Major signal increase in fluorescence microscopy through dark-state relaxation. *Nat Methods* **4**, 81-86, doi:10.1038/nmeth986 (2007).
65 Elson, E. L. Fluorescence correlation spectroscopy: past, present, future. *Biophys J* **101**, 2855-2870, doi:10.1016/j.bpj.2011.11.012 (2011).
66 Kuznetsov, A. V. *et al.* Mitochondrial ROS production under cellular stress: comparison of different detection methods. *Anal Bioanal Chem* **400**, 2383-2390, doi:10.1007/s00216-011-4764-2 (2011).
67 Duffy, P. A. Cell culture phototoxicity test. *Methods Mol Biol* **43**, 219-226, doi:10.1385/0-89603-282-5:219 (1995).
68 Jacques, V. *et al.* Enhancing single-molecule photostability by optical feedback from quantum jump detection. *Applied Physics Letters* **93** (2008).
69 Byrdin, M., Duan, C., Bourgeois, D. & Brettel, K. A Long-Lived Triplet State Is the Entrance Gateway to Oxidative Photochemistry in Green Fluorescent Proteins. *J Am Chem Soc* **140**, 2897-2905, doi:10.1021/jacs.7b12755 (2018).
70 Resch-Genger, U., Grabolle, M., Cavaliere-Jaricot, S., Nitschke, R. & Nann, T. Quantum dots versus organic dyes as fluorescent labels. *Nat Methods* **5**, 763-775, doi:10.1038/nmeth.1248 (2008).